THE AMBIENT ELECTROMAGNETIC ENVIRONMENT IN METROPOLITAN HOSPITALS

Philippe Boisvert, B.Eng. (McGill)

A thesis submitted to the Faculty of Graduate Studies and Research in partial fulfillment of the requirements for the degree of Master of Engineering

Department of Electrical Engineering
McGill University, Montreal
May 1991

Abstract

Electric field levels between 30 and 1000 MHz were predicted using a free space propagation model, and then measured in three major hospitals in downtown Montreal. The measurements were performed using industry-standard techniques and new broadband, omnidirectional, triaxial, electrically small (BOTES) techniques. Although the absolute values of predictions were often unreliable, they acceptably predicted the type of electromagnetic environment actually observed at different hospitals. Results from both sets of measurements were closely related, suggesting continued future development of lower-cost BOTES measurement techniques. None of the fields encountered were above the limit prescribed by the Food and Drug Administration (FDA) susceptibility standard for medical devices. Correlations of survey results and of previous reports of device malfunctions in the rooms surveyed suggest that compliance with the FDA standard should be mandatory rather than voluntary. Results obtained by industry-standard techniques were used to simulate the effect of measured electromagnetic environments on typical biomedical equipment, and the simulations show that disruptions of the normal operation of medical devices are to be expected.

Résumé

Les champs électriques entre 30 et 1000 MHz ont été calculés, à partir de données obtenues du Ministère des Communications, au moyen du modèle de propagation d'onde "champs libre", pour trois hôpitaux importants de Montréal. Ensuite, les mêmes champs ont été mesurés de deux façons: a) en utilisant une méthode et des appareils reconnus et b) en utilisant une nouvelle méthode axée sur une antenne triaxiale, omnidirectionnelle, électriquement petite et à bande passante large, baptisée BOTES. Même si la valeur absolue des champs calculés n'était pas fiable, ces calculs ont néanmoins fourni une bonne indication de l'intensité de l'environnement électromagnétique dans les trois hôpitaux. Les résultats des deux types de mesures sont très semblables, ce qui suggère un effort de développement de l'antenne BOTES plus poussé. Aucun des champs mesurés ou calculés ne dépassait les limites de susceptibilité électromagnétique établies par la norme régissant la compatibilité électromagnétique des appareils médicaux, publiée par la Food and Drug Administration (FDA). Les résultats obtenus, de concert avec la documentation sur les bris précédents d'appareils médicaux, suggèrent que la conformité avec la norme de la FDA soit obligatoire plutôt que volontaire. Trois distributions spectrales des champs electriques mesurés au moyen de techniques et instruments reconnus ont éte utilisées pour simuler l'effet de l'environnement électromagnétique sur des instruments médicaux typiques. Les resultats de cette simulation montrent qu'il est possible que l'environnement, tel que mesuré, fasse obstacle au bon fonctionnement de l'appareil.

Acknowledgements

The author wishes to espress sincere gratitude to Professors T.J.F. Pavlasek and B.N. Segal for their continued support and encouragement and their valuable guidance.

Thanks are also due to the heads of the Biomedical Engineering departments of the five teaching hospitals affiliated with McGill University for their cooperation before and during the experiment.

The participation of the Department of Communications is gratefully acknowledged, for its contribution of data on local transmitters and for its assistance with the measurements.

Thanks are due to the Department of National Defence for its involvement with the experiment.

Finally, the author would like to thank Evelyn LaRoche, Ginette Jacques and Michel Boisvert, whose encouragement and understanding made this work possible.

The support of this work by a grant from the Department of Health and Welfare is gratefully acknowledged.

Table of Contents

Table of Figures

Table of Tables

Chapter 1 INTRODUCTION

Recent decades have witnessed rapid growth in the use of the electromagnetic spectrum, and this growth has intensified in recent years. Meanwhile, medical devices have become more intricate, in that they must now perform complex tasks automatically, as a consequence of advances in digital technology. In addition, the microcircuitry technology used is delicate and susceptible to malfunction and damage in a hostile environment. These three factors, in combination with the fact that shielding poses major technical and operational problems, for example in the case of the electrode lead which connects the patient to an instrument, have led to an increasing concern regarding the safety and the reliability of medical equipment in the existing electromagnetic environment (EME). Similar concerns led to several studies in the early 70's [1][2][3][4] which provided a basis for an electromagnetic compatibility standard for medical devices [5], published in 1979 Eight years after the publication of the standard, there nevertheless existed continuing and growing concern over the electromagnetic interference situation in hospitals. As a consequence, the Department of Health and Welfare Canada organized a workshop on Electromagnetic Interference (EMI) and Electromagnetic Compatibility (EMC) in Health Care Facilities in Edmonton , Alberta [6]. This workshop resulted in several recommendations, including the proposal for:

> - the establishment of "A cross Canada survey of EMI/EMC problems and solutions and data base development. The purpose for this is to enlarge and make more meaningful the database on EMI/EMC problems and solutions which have been experienced within Canadian Hospitals", and a suggestion that
> - "at least one major center be examined in detail as part of the process by which a comprehensive survey is conducted across Canada. Also it is recommended that data on EMI/EMC incidents be collected on an on-going basis from individual hospitals and other relevant sources."

The McGill Biomedical Group on EMC was formed in response to these recommendations. It consists of the heads of the biomedical engineering departments of the five teaching hospitals affiliated with McGill University, a professor of biomedical engineering

and a professor of electrical engineering. The five teaching hospitals affiliated with McGill University are the Montreal General, the Montreal Children's, the Jewish General, the Royal Victoria and Saint-Mary's hospitals. The purpose of the group is:

- to define a medical equipment failure database
- to document past and present EMI-related malfunctions using the database
- to perform an electromagnetic survey from 30 to 1000 MHz of the areas where medical equipment has malfunctioned due to EMI. The investigation would be limited to this range of frequencies because previous urban measurements estimate that most high field strengths are in that band.

This thesis concerns itself with the last objective, divided in four steps. Chapter 2 deals with the first phase of the survey, namely predictions. As an estimate of the ambient electromagnetic environment, the electric field levels created by known, fixed and documented sources operating between 30 and 1000 MHz in the neighborhood of the hospitals were calculated using a free space propagation model. These calculations were repeated for each floor of three of the five hospitals. They showed that the free space propagation model predicted little variation in field strength from floor to floor. The calculations also allowed the hospitals to be ranked according to electromagnetic environment hostility (A, B, C, D and E, A being the most hostile and E the least). Also, the calculations showed that the strongest fields in any given location would be those from broadcast TV or FM towers and that all the expected field levels were below the susceptibility limits set by [5], which states that the performance medical devices should not be affected by E field levels less than 133 dBμV/m for frequencies between 30 and 470 MHz or less than 137 dBμV/m for frequencies between 470 and 1000 MHz. Finally, the Equivalent Electric Field (EEF) was defined as the square root of the sum of the squares of the field levels in a given band. This definition is similar to the impact factor described in [4], but differs in application. Whereas [4] used a single EEF to describe the entire EME in a location, the McGill group used 4 or 5 EEFs. This preserved the outline of the spectral distribution and still provided information on the intensity of the environment.

Chapter 3 deals with the second phase of the survey, namely measurements. Based on the values of the predicted E fields and on the geographic layout of the buildings, three hospitals were chosen for the site surveys: hospitals A, C and D Electric field strengths between 30 and 1000 MHz were measured by the Department of Communications Canada (DoC) using industry standard equipment and methods [7] The McGill Biomedical Engineering Group on EMC experimented with a new way of measuring the electromagnetic environment using innovative BOTES (Broadband, Omnidirectional, Triaxial, Electrically Small) equipment developed by the author. The Department of National Defence provided an additional signal in a sparsely used region of the spectrum of interest. The results of these measurements show that, as was predicted by the calculations of chapter 2, hospital A indeed has the worst EME of the three hospitals, followed by hospital C and hospital D. The results also show as predicted in chapter 2, that the strongest signals recorded are those from broadcast TV and FM transmitters. Finally, none of the spectral distributions rose above the susceptibility threshold specified in [5].

Chapter 4 is an analysis of the results gathered in chapters 2 and 3. First, the predicted field levels presented in chapter 2 are compared to the field levels measured by DOC using standard techniques. Occasionally the measured field levels were higher than the predictions, but most often, the predicted field levels exceeded the measurements by 20 to 60 dB These large discrepancies are mainly attributable to the difference between the measured fields of inactive mobile communication channels (i.e. the noise level of the spectrum analyzer) and the predicted fields of active channels. The differences between the predicted and measured values are of course due to the inherent simplicity of the theoretical propagation model used and the extreme complexity and substantial unpredictability of the urban propagation environment. However, the simple free space propagation values serve, as usual, as a basic reference datum. The practical result of the measurements obtained is to provide a guideline for the additional signal attenuation to be expected. These results indicate additional attenuation of 20 dB for direct line of sight and 30 dB attenuation for shadowed path conditions.

Next, the measurements performed with DOC's standard equipment and techniques were compared to the McGill Group's new BOTES method The results are similar, having a mean difference of less than 1 dB, a standard deviation of 8 dB and a correlation factor of .86. The plot of standard deviation as a function of frequency falls within the acceptable levels reported in [8]. Chapter 4 concludes with an attempt to define the EME in which medical equipment is most likely to malfunction due to EMI However, the description of the environment in which a device will malfunction depends heavily on the device itself Therefore, one single spectral distribution (EME) could not describe the entire range of situations. Nevertheless, it was noted that relocating malfunctioning instruments to rooms where the EEF in the FM band was 10 to 15 dB lower than in the original location usually solved the problem.

As the study proceeded, it began to yield results which, in addition to assessing the EME levels, provided an opportunity to attempt a preliminary examination of how such an environment might affect a potential EMI victim. Such a preliminary study is presented in chapter 5. The results of chapter 3 are used to simulate the effect of a hostile EME on typical biomedical equipment. One industry standard measured spectral distribution from each of the three hospitals surveyed in chapter 3 is used to calculate the voltages induced on an unshielded electrode lead, which typically connects a patient to some equipment The progressive effect of these voltages at various stages of the medical device is simulated. The results show that a hostile EME of the type measured in this study might disrupt the proper operation of ordinary medical instruments This simulation was carried out assuming linear behavior of such equipment and must be considered preliminary to another separate extensive study. In such a study, the failure modes of equipment would be examined both by simulation and experiment and would consider a broad range of factors.

Chapter 6 is a summary of the conclusions drawn from each of the chapters, which in brief state that the free space propagation model is poor for absolute values of electric field, but acceptable as a relative indicator of environment hostility (chapter 2), that the EMC standard for medical devices should be made mandatory (chapter 3) and that, on the average, the industry standard and BOTES methods produce similar results, even though

individual outcomes are always different (chapter 4). Chapter 4 also states that it is difficult to describe quantitatively the EME in which devices malfunction. However, it indicated that, as a guideline, a 10 to 15 dB reduction in the EEF of the FM band from a malfunction inducing condition will ensure proper operation. Chapter 5 demonstrates that some of the measured environments might interfere with the proper operation of medical devices.

Appendix A a is detailed description of the design of the BOTES probe. The electrical behavior, impedance and antenna factor of electrically small dipoles are calculated. The triaxial feeding arrangement based on the BIRES [9] probe is described, as well as the balun. The antenna's omnidirectionality characteristic is proved in [9].

Appendix B consists of table of the EEFs in each surveyed location, along with a short description of the health care use of the site and a note when equipment has malfunctioned.

Chapter 2 PREDICTED ELECTRIC FIELD LEVELS

2.1 General

This chapter describes the calculations made to estimate the predicted field levels at each hospital. This formed an early stage of the project and was also important as a basis for making a choice of the hospital sites to be surveyed. Since equipment, manpower and time resources were available for making only three preliminary surveys, theoretical predictions of the electric fields on the top floor of each of the five teaching hospitals were calculated to help decide which three of the five hospitals would be the subjects of the preliminary study. These estimates, combined with the number of reported malfunctions attributed to electromagnetic interference (EMI) and with practical considerations for moving the measurement equipment, narrowed the field down to three hospitals: hospital A, hospital C and hospital D. In order to estimate the electromagnetic environment, theoretical electric field strengths were calculated for every floor of each building.

This chapter describes the propagation model chosen, outlines the calculation method, presents the results of the predictions and defines the Equivalent Electric Field.

2.2 Propagation Model

Free space propagation was assumed for all calculations, although all three buildings lie in a complex urban environment. Such calculations serve as benchmark indicators and are especially useful for indicating the relative strengths at the various sites.

A first improvement over the basic free space model would be to take into account the effect other nearby buildings have on the field levels at each hospital. This would imply calculating the attenuation, scattering and reflections due to single buildings and to clusters of buildings of differing heights, structural materials ans shapes. Because of the extreme complexity of the urban physical environment, such calculations are unlikely to be deterministically tractable.

The second aspect of modeling would consider the effect that the structure of the building under study has on its own internal fields. This could be extended to include the effect of large metallic furnishings and equipment. The attempt at such calculations again presents a challenging problem, requiring a major study in its own right.

A third separate issue of the propagation problem in making estimates of the field levels would be to consider the time dependance of the signals under study. This includes not only the temporal behavior of a propagation path but also the behavior of the source. For example, the probability that a cellular telephone channel is in use varies with the time of day, such that the electric field produced is no longer only a function of position with respect to source, but also a function of time in the short term, horary, daily and longer term basis.

If the first two improvements mentioned above were manageable, they would involve an immense and complex computer simulation for each emitter pertinent for each room of each hospital. Since the rooms that would be surveyed cannot be known a priori due to the emergency nature of their use, all the relevant rooms would have to be examined, for a total of

330 frequencies x 25 rooms x 3 hospitals = 25000 simulations

Clearly, both the nature of such calculations and the magnitude of such a task are beyond the scope of a preliminary study with limited time and computing power, and therefore free space modeling is the only appropriate option.

2.3 Evaluation of E field levels

2.3.1 Methods

The information needed to calculate the electric fields at the three hospitals was obtained from three sources.

The Department of Communications (DoC) provided a list of all the fixed, known and documented radiators in the 30 to 1000 MHz band that were within about one kilometer of each hospital. For each frequency, five parameters were given:

-Effective Radiated Power (ERP= power radiated x gain of antenna); in dBW
-Antenna pattern
-Position (longitude, latitude and altitude)

The Department of National Defense provided a similar unclassified list of transmitter parameters.

The geographic information was obtained from a 1 : 20000 map of Montreal issued by the department of Energy and Resources of the provincial government of Quebec. It was used to find the position of the three hospitals with an accuracy of 10 meters in longitude and latitude and 5 meters in elevation.

The antenna radiation pattern and the three dimensional displacement vector locating the hospital location with respect to the source were used to determine the free space predicted field at each location.

2.3.2 Results

The results are presented in Fig. 2.1, where the mean value of the electric field is represented by a horizontal bar while the vertical lines represent two standard deviations, one above and the other below the mean. Four characteristics are evident: a) the predicted fields showed little deviation from average, b) the strongest fields expected were those of TV and FM high power transmitters, c) there was a scarcity of signals in the 225 to 400 MHz and the 500-800 MHz bands and d) all expected field levels were well below the standard which regulates the immunity of medical devices [5]. This standard sets at 133 dBμV/m the susceptibility limit of medical devices between 30 and 470 MHz and at 137 dBμV/m between 470 and 1000 MHz, and is represented in the graph by a dashed horizontal line.

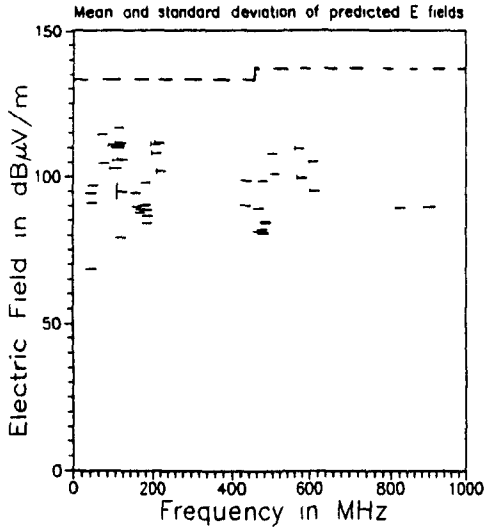

a) Hospital D

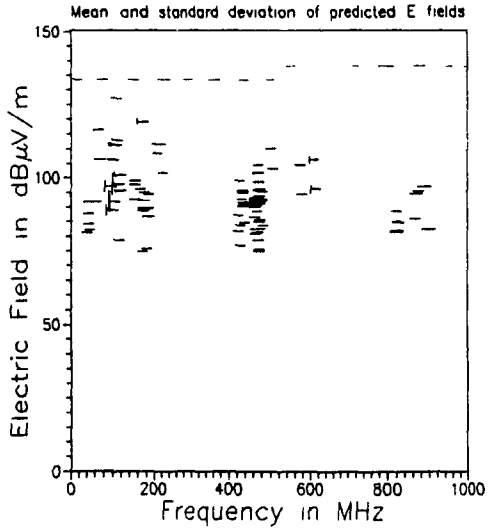

b) Hospital C

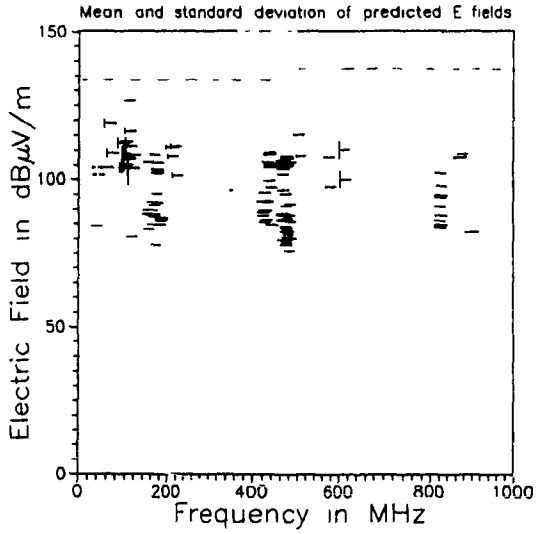

c) Hospital A

Figure 2.1 Predicted electric field levels

2.3.3 Discussion of results

The effect of building height on the field levels was of concern, but because the angle subtended by each hospital was small, the predicted fields of Fig. 2.1 had

small standard deviations. Figure 2.2 illustrates the typical situation of a 50 meter high building, located 100 meters above sea level, facing a source on a tower 100 meters high, located at the peak of a 230 meter mountain.

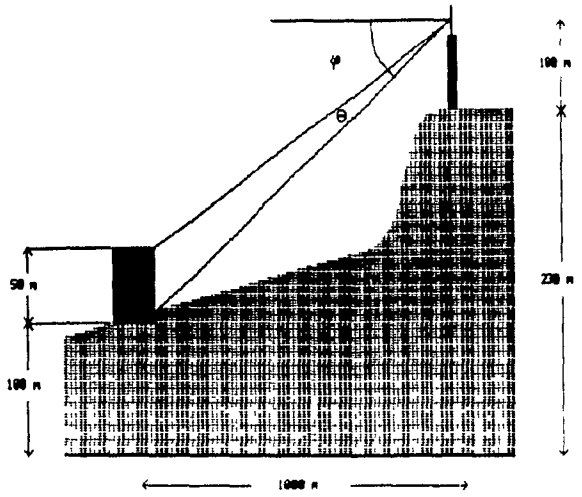

Figure 2.2 Angle subtended by a typical building in downtown Montreal

The angle θ subtended by the hospital was in this case 1.8°. None of the radiation patterns studied varied greatly over 1.8°, which explains the small standard deviations of Fig. 2.1. However, should a building be in the direction of an elevation pattern null, the effect could be substantial. Such conditions did not prevail here but have been observed in the case of other buildings [10].

The scarcity of signals encountered in the 225 to 400 MHz and the 500-800 MHz bands was expected because these frequencies are assigned mostly for military purposes or reserved, but not yet exploited, for broadcast use. Therefore, these bands remain largely unused.

2.4 Equivalent Electric Field

In direct contrast to the sparse use of the above mentioned bands, the overpopulation of other bands is apparent, especially the 800 to 900 MHz region, reserved for mobile

cellular communications. This has prompted the use of a tool whose purpose is to formulate an estimate of the power in a given band. Here it is labeled Equivalent Electric Field (EEF), it is defined as *the electric field which would result from a source producing as much power density as the sum of the power densities in a given band*, or

$$EEF = \sqrt{\sum_{f_i=f_L}^{f_U} E(f_i)}$$

where $E(f_i)$ is the electric field of source *i* radiating at frequency f_i, and f_L and f_U are the lower and upper limits of the band under study.

The predicted Equivalent Electric Fields for certain bands at the three hospitals are presented in table 2.1.

Table 2.1 Predicted Equivalent Electric Field in dBμV/m

Band	Hosp A	Hosp C	Hosp D
0-30 MHz	106	107	106
30-50 MHz	108	96	100
88-108 MHz	128	128	121
138-174 MHz	115	121	102
400-470 MHz	122	112	103
806-890 MHz	120	114	105

Chapter 3 MEASURED ELECTRIC FIELD LEVELS

3.1 General

This chapter describes how ambient electric field levels between 30 MHz and 1000 MHz were measured in six locations in and near hospital D, eight at hospital C and seven at hospital A. At each hospital, one survey was performed outside, near the main entrance facing the tower on top of Mount Royal, and the rest took place indoors. The inside measurements were conducted in rooms where there were reported malfunctions attributed to EMI, in critical care rooms where most of the electronic biomedical instrumentation is concentrated, in laboratories where highly sensitive and sophisticated computer controlled equipment is used and finally in future sites of critical care or special facilities rooms, such as the future site of an MRI (Magnetic Resonance Imaging) machine.

This chapter describes the techniques and the equipment used, presents preliminary results of the survey and situates these results with respect to the EMC standard for medical devices.

3.2 Methods

3.2.1 Methods of measurement

The measurement of the ambient electromagnetic environment (EME) in the three hospitals involved the simultaneous activities of three teams. The first team would generate an additional reference signal while the two other teams would measure the environment, (a) with standard methods and equipment and (b) with new methods and innovative equipment.

3.2.1.1 The reference signal

The task of the Department of National Defense (DND) was to radiate a continuous wave (CW) signal in one of the empty bands mentioned in section 2.3.3. This signal was needed for three reasons: first, it fills a void in the spectrum,

as there are usually no emitters in the 225-400 MHz band. Secondly, the signal produced by DND would be unmodulated and its operation would be under the measuring teams' control, thereby providing a stable means of reference for comparison purposes. Lastly, the emission of this signal would give an indication of the impact a new mobile communications tower might have on the EME in hospitals.

The DND equipment used consisted of a mobile communications truck, configured to feed a corner reflector antenna with a 290 MHz, 100 watt sine wave. The apparatus was installed on premises owned by the DND, so as not to interfere with traffic and to comply with DOC regulations. For the measurements at hospital D, the DND signal originated from the Armory on Cotes Des Neiges, 2000 meters away. During the measurements at hospitals C and A, the truck was moved to the St-Sulpice Road Montreal DHQ, 750 meters from hospital C and 500 meters from hospital A. In each case, the antenna pattern's main lobe was directed towards the hospital.

3.2.1.2 Standard methods and equipment

The purpose of the Department of Communications (DoC) participation was to measure the EME (including the signal from the Department of Defense) both inside and outside the three hospitals. The DoC used IEEE industry standard site survey techniques [7] which require costly equipment otherwise unavailable to the McGill Group and would lend the results of the preliminary study the weight and reliability associated with an official authority.

The equipment used consisted of a folding biconical antenna, model SAS-200/542 from A.H. Systems for the frequency range of 30 MHz to 300 MHz, and a broadband circuit board antenna, model 91597-2 from RI-FI Measuring Equipment for the measurements from 300 to 1000 MHz. The receiver was a spectrum analyzer, model A7550 from IFR Systems, interfaced to a laptop computer for data acquisition and control.

For each room, the entirely automated system separated the 30-1000 MHz range into 40 subranges:

- 2 subranges of 100 MHz each to cover the 200-400 MHz band,
- 2, 6, 7 and 19 subranges of 10 MHz each to cover the 30-50 MHz, 110-170 MHz, 400-470 MHz and 800-990 MHz bands, respectively,
- 4 subranges for broadcast transmitters.

Each one of the first 36 subranges above was swept 10 times with a resolution bandwidth of 25 kHz (or 250 kHz for the 100 MHz ranges), and only the largest value in each 25 kHz (250 kHz) slot was retained. These measurements were taken with the antennas in the vertical position.

The last four subranges dealt with the TV and FM broadcasters. For each FM station, the system measured the maximum amplitude over a 10 second interval in horizontal polarization. Then the system repeated the measurements for the vertical polarization. The attention given to TV signals was the same, except that measurements were only taken in horizontal position. For all measurements made in the horizontal polarization the antennas were oriented so as to give the strongest signals.

For each room, the laptop computer produced 40 files (one for each subrange) in approximately 25 minutes. Thirty six of those were sweeps of subranges, two were for FM (one horizontal and one vertical) and the last two were for TV stations, grouped in one file for VHF and another for UHF. In general, for inside measurements, the antennas were placed near windows, because that proved least disruptive to the hospital staff. For outside measurements, the antennas were mounted on a telescoping tower about 15 meters from the main entrance and were raised to an equivalent height of three floors (10 meters).

The three days of measurements produced approximately 8 Mbytes of raw data in 840 files (21 sites x 40 files per site) containing the raw output from the spectrum analyzer, in dBm. Several steps were taken to convert this data into coherent, presentable information. First, these 840 files were concatenated to produce 21 files (one for each surveyed site) of the spectrum analyzer's output. The data in these files was plotted in raw form to allow rapid error checking with subsequently altered data. Then, the data was converted from dBm to dBμV/m by:

$$E(dB\mu V/m) = Signal Amplitude(dBm) + 107 + Antenna Factor + Loss$$

where the 107 dB constant comes from the conversion of dBm to dBμV, assuming a 50 Ω load. The Antenna Factor was extracted from the antennas' specifications, which provided values for frequency steps of 10 MHz. Since the measurements were taken in much finer intervals, a linear interpolation scheme was used to obtain the antenna factor for any frequency. Finally, the loss due to cables was given by $\frac{f}{125\times10^6}$(in dB) for exterior measurements and by $\frac{f}{500\times10^6}$(in dB) for interior measurements.

3.2.1.3 BOTES methods

The McGill Biomedical Group on EMC aimed to measure the EME in hospitals on a continuing basis. To enable the McGill group to make reliable preliminary surveys in potentially troublesome areas without the assistance of DoC, the design of a proper receiving antenna was called for. The requirements were the following:

- the receiving system should be small because of the typical lack of space in hospitals
- the antenna would have to be electrically small so as not to interfere with the field structure
- the probe should handle moderately high field strengths (130

$dB_{\mu}V/m$)

- the antenna should have good working characteristics over the entire band of interest, 10 to 1000 MHz
- because the measurements would be performed inside buildings, the polarization of the wave would be difficult to determine, thereby requiring that measurements be made in three orthogonal polarizations
- and lastly, because the signals could come from any direction, the probe would have to be omnidirectional.

Thus the BOTES (Broadband, Omnidirectional, Triaxial, Electrically Small) E field probe was designed and built. Its design is presented in more detail in Appendix A. For this survey, it was used with a spectrum analyzer, model 2710 from Tektronix, connected to a dot matrix printer for hardcopy Each of the probe's three polarizations were scanned for non commuted signals, i.e. the broadcasters and the DND signal, and the spectrum analyzer recorded only the maximum amplitude of each trace in a 2 minute interval. In each room, it took an hour to measure and print all 27 signals (14 TV signals from 7 stations, 12 FM stations and one from DND) for all three polarizations. Consequently, fewer rooms were investigated with the BOTES method than with the standard method.

In general, the probe was positioned where the signals were the strongest, which often meant taping it to a window facing the tower on Mount Royal. While searching for maximum field levels, it was found that levels were lower behind the portion of a window with metallic screening, prompting the suggestion that windows should be fully screened for maximum attenuation. In hospital D, the combination of low signals and poor antenna factor were enough to warrant the use of the spectrum analyzer's 12 dB preamplifier, and in all rooms except one, the maximum field intensity was measured by searching for the largest signals in any polarization. In the other two hospitals however, the signals were strong enough to be recorded for all three polarizations. At hospital C, this was done

by connecting a cable to one of the probe's outputs and by rotating the probe 120° about its axis. At hospital A three cables were connected to the probe (one for each termination) and each of the three antennas' signal was recorded alternately. The last methodology allowed the probe to be fixed for the duration of the survey in a room.

After the measurements were completed, the BOTES data was digitized manually from the plots generated by the spectrum analyzer. Thirteen files were thus created. They were converted from dBm to μV, the three polarizations were combined vectorially and the antenna factor was added to produce E field levels in dbμV/m in one single step, using a popular spreadsheet software. Then, the results were plotted.

3.3 Results of the survey

The raw results of the survey consist of 34 graphs of the type shown in Fig. 3.1 and 3.2, which represent the EME in an equipment-filled critical care area on the fourteenth floor of hospital A, as measured by standard and BOTES methods, respectively.

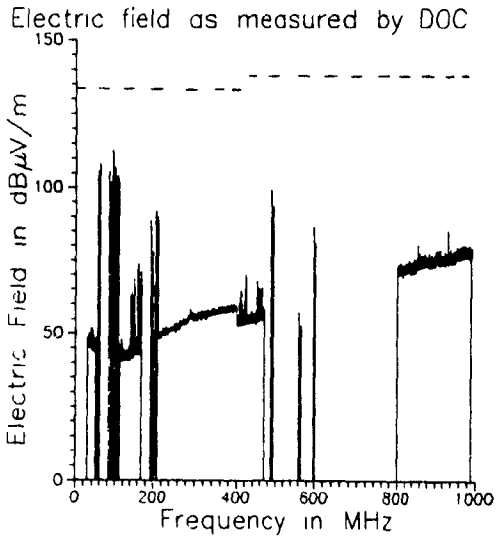

Figure 3.1 Standard method

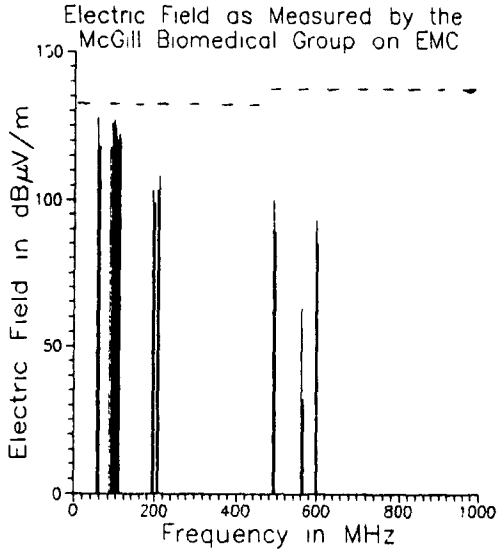

Figure 3.2 BOTES method

As was predicted in chapter 2, the strongest signals in Fig. 3 1 were those from broadcast transmitters (the strong signals in pairs are television stations, and the high level group around 100 MHz is the FM band). The 100 watt signal from the DND transmitter 500 meters away does not appear in this graph because the transmitter was not turned on during this particular measurement The sloped noise level comes from the fact that the noise level on the spectrum analyzer was not adjusted to compensate for the frequency dependance of the antennas and the loss factors. While levels for this room are moderate, field strengths as high as 135 dbμV/m were measured during the survey.

When Fig 3.2 is compared to Fig. 3.1, two features are immediately apparent: there are fewer points due to the longer duration of the BOTES measurements and while the signal levels are different, they do show a similar relative trend. That the signal levels be different is disturbing at first, but as will be seen in chapter 4, discrepancies are to be expected and can be explained to some extent.

The following comments can be made about the ensemble of these graphs. First, the strongest fields are always those from TV and FM transmitters. These produce levels well above 100 dbμV/m and can reach 135 dBμV/m in some instances even though the measurement sites were well out of the main lobes of the transmitting antennas. By comparison, the fields produced by the 100 watt DND transmitter, whose antenna was aimed directly at the hospitals varied from 40 to 80 dBμV/m, even though it was closer to the measurement sites. Prorating the DND power level upwards to levels corresponding to the TV and FM stations would increase these levels 20-30 dB, for a total of 60 to 110 dBμV/m. These levels are still lower than those from broadcast stations, probably because the latter enjoyed a clearer path to the measurement site.

Secondly, because it generally did not enjoy a line of sight type of propagation and because it was the farthest hospital from most broadcast transmitters, hospital D was subject to lower field levels than the two other hospitals surveyed. The lowest ambient levels were recorded in a new wing of hospital D (see the EEF values in table B.5 in Appendix B), although this site was reasonably well exposed to the broadcast

transmitters. Fields were lower there apparently because the vapor barrier used in the building's construction is metallic rather than plastic, thus providing a rudimentary form of shielding.

Thirdly, none of the field strengths measured by either method were above the limits set by the Electromagnetic Compatibility Standard for Medical Devices produced by the Food and Drug Administration mentioned in chapter 2. According to this document, the maximum field strengths up to which medical devices must not show an unacceptable degradation in performance is 133 dBμV/m from 30 to 470 MHz and 137 dBμV/m from 470 to 1000 MHz. No specifications have been made above 1 GHz. The fact that there have been malfunctions attributed to EMI in some of the rooms that have been surveyed in this preliminary study indicates the possibility that the standard is not being met, since the levels measured were below the susceptibility limit and therefore should not have caused any unacceptable malfunctions. At the same time, the results of this experiment suggest that the standard should not only be reviewed, since the ambient EME has considerably changed since the measurements on which the standard is based were made in 1975, but it should also be changed from a voluntary to a mandatory one, given the possible consequences of a malfunction in a health care setting.

To summarize the results, the mean and standard deviation of the field levels were calculated for the bands of table 2.1 (30-50 MHz, 138-174 MHz, 400-470 MHz, 806-890 MHz, 88-108 MHz), where most of the activity was predicted and where documentation of sources was available. Leaving out the rest of the measured spectral distribution is a valid approximation since no signals were recorded outside these bounds except the DND signal. The graphs of the mean and the standard deviation of the fields measured at each hospital by both methods are presented in Fig. 3.3 and 3.4. As before, the mean value of the electric field at a particular frequency is indicated by a horizontal bar while the associated vertical line represents the standard deviation from the mean.

Because DoC automated measurement system attempted to set the optimal sensitivity for each 10 MHz (100 MHz) sweep in each room, and because it did not consistently use the same settings for each site of any of the three hospitals, the noise levels varied

from room to room, resulting in a mean noise level with a large standard deviation. However, this does not impede the detection of active channels, as these are readily observable in Fig. 3.3. On the other hand, the height of the noise level poses a severe obstacle to the detection of active channels. This could be remedied by simply lowering the attenuation on the spectrum analyzer such that the true EME could be measured, rather than the instrument's minimum recordable value.

Upon closer examination, one could detect larger standard deviations of the broadcast signals at hospital D. This is due to the more eclectic choice of rooms surveyed there, ranging from the lowest intensities to slightly above average. At hospital D, another phenomenon occurs: as the broadcast signals decrease because of the increased distance from the broadcast towers, their field levels become comparable to those of the other bands, which are used mainly for mobile communications.

In comparison to hospital D, hospital A is a hostile EME. Its fields are much higher, especially in the FM band. With few possible exceptions, it is the worst ambient electromagnetic environment in which sensitive instruments must operate in the Montreal area.

Finally, it will be observed from Fig. 3.3 and 3.4 that there is a noticeable difference between the results of the standard measurements and the BOTES measurements. Substantial differences also appear between the EEFs of each room presented in Appendix B, which contains tables of EEFs for each of the rooms surveyed, as mentioned in the introduction. These discrepancies are examined further in chapter 4.

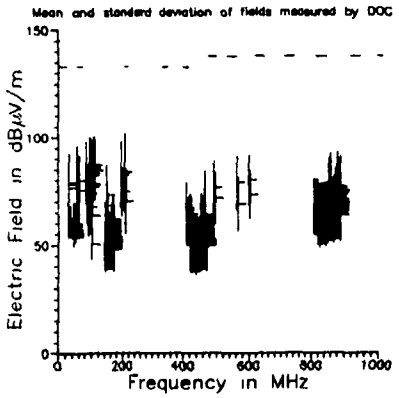

a) Hospital D

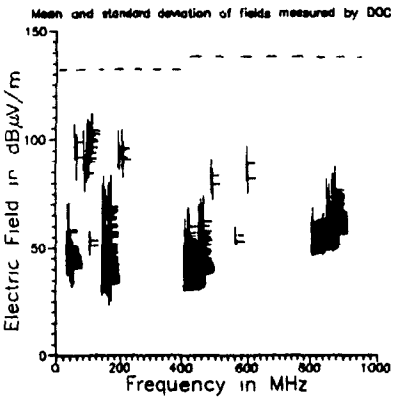

b) Hospital C

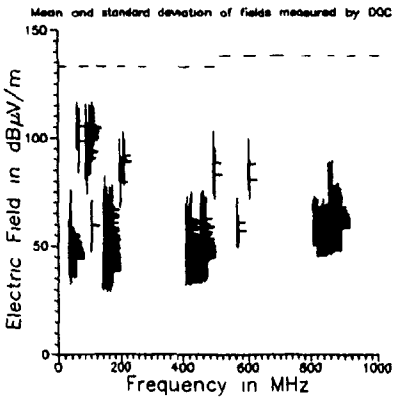

c) Hospital A

Figure 3.3 Mean and standard deviation of fields measured by DoC

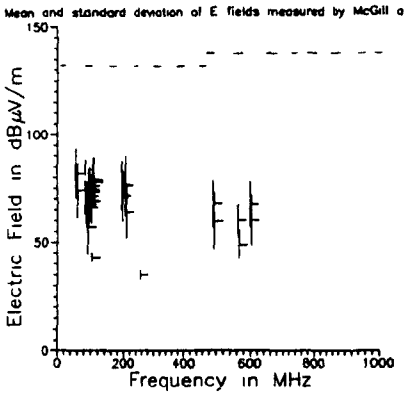

a) Hospital D

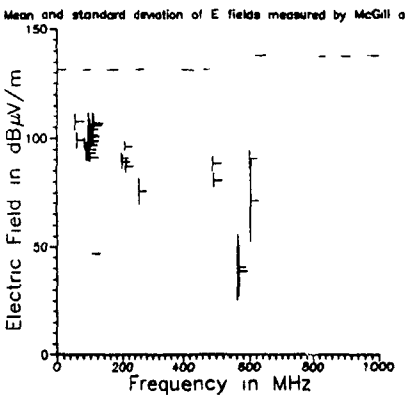

b) Hospital C

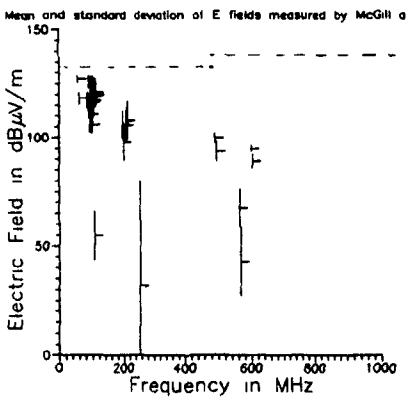

c) Hospital A

Figure 3.4 Mean and standard deviation of fields measured by McGill

3.4 Discussion of method of measurement

Because the goal of this preliminary study was primarily to estimate the EME in hospitals and to develop the tools to do so efficiently, the method of measurement was rather crude and to the point. By comparison, the Recommended Practice For An Electromagnetic Site Survey [7], describes a more extensive process. The key elements were nevertheless retained, such as the recommended use of a biconical dipole for measurements between 30 and 300 MHz and the use of photographs to record the exact location of the measuring equipment and the surrounding environment.

Unfortunately, most of the "recommended practices" could not be followed either because of space or time constraints or lack of equipment. Space constraints were due to the typical lack of floor space in hospitals, which prevented the placement of antennas in the middle of the rooms, as recommended.

The time constraint caused by the tight schedule (21 surveys in three days) was the most severe limiting factor. It prevented each site from being measured exhaustively, i.e. one survey per hour during 14 days, and also prevented each building from being surveyed in keeping with the standard. The recommended practice for surveys inside buildings requires measurements at each corner of each floor (including the basement) at varying distances from the outside walls, from windows to doorways. For the three hospitals, which have a total of 36 floors and 144 corners, this would mean a minimum of 300 independent 14 day surveys. Were the measurements carried out consecutively, such a massive survey would last more than ten years; done concurrently, with faster, more sophisticated equipment, the experiments might be done in a year and a half.

Even more equipment would be needed to follow the recommendation of monitoring the bands of interest with headphones while measuring, to ensure that there are no abnormalities. The standard also advises calibrating the measurement system in laboratory both before and after the survey. This was not done for either of the two systems because no facilities were available for such calibrations. Finally, still more equipment would be necessary to check all ground points of the measuring instruments, as recommended.

Although pessimistic in appearance, the comparison between the state of the art in measurement practice and the way the survey was carried out does not point to errors but to improvements. The method of measurement used in the preliminary study was not perfect but still very adequate. In fact, perfect compliance with the recommended practice would require following questionable policies, like the recommended use of antennas which are large compared with the dimensions of the areas in which they are supposed to work: the biconical antennas recommended for measurements between 30 and 300 MHz are more than 1 meter long and severely affect fields in areas where the distance between large metallic objects is 2 meters. In addition to the effect that the antenna has on the surrounding fields, the effect of the surroundings on the pattern and impedance of the antenna must be considered. Therefore, the meaning of the output from such an antenna in such a position is cause for concern, as indicated in [11]. Also, the recommended practice of measuring only one polarization inside buildings is questionable. Elementary field theory predicts that any singly polarized wave incident on a metallic structure as complex as that of a building will become multiply polarized inside the structure. Lastly, the recommended use of a log periodic antenna for indoor measurements between 200 MHz and 10 GHz should be reviewed, given the directional pattern of such an antenna. Regardless of its shortcomings, the Recommended Practice for an Electromagnetic Site Survey remains the most complete guide available. The measurements for the full blown study should follow more of its valid recommendations, avoid its weaknesses, involve more buildings, more internal and external locations and extend over longer periods of time. In sum however the resulting time required and the level of effort involved to carry out a full blown survey in keeping with the recommended practice indicate that as presently formulated, such a survey would be an essentially inappropriate approach to the problem.

Chapter 4 ANALYSIS

4.1 General

This chapter presents the analysis of the results of the experiment. The goals were: (a) to assess the usefulness of the propagation model by comparing predicted fields to measured values, (b) to assess the reliability of the McGill measurement system by comparing its results to DoC's and (c), in light of the field levels observed in chapter 3, to assess the electromagnetic characteristics that may lead to EMI malfunctions in a given room.

4.2 Differences between the measurements and the predictions

The differences between predicted and measured field levels of documented sources ($E_{predicted} - E_{measured}$) were calculated for each measurement site. These discrepancies were then processed to obtain a graph for each hospital showing the mean and standard deviation of the difference $E_{predicted} - E_{measured}$ as a function of frequency. These graphs are presented in Fig. 4.1. Of note are the large differences expected in those channels which are commuted (as opposed to those which radiate continually) and not active, as was the case for mobile communications channels below 50 MHz, around 150 MHz, around 450 MHz and around 850 MHz. It may be recalled that the predicted field strengths of chapter 2 assumed all channels to be active, and one of the propagation model's shortcomings was that it did not provide a mean or most probable amplitude for commuted signals. The large values in Fig. 4.1 can thus be explained as being the difference between the predicted fields of an active channel and the noise level of the spectrum analyzer. On the other hand, mobile communications channels that were active during measurements readily stand out because the difference between $E_{predicted}$ and $E_{measured}$ levels is less (for example, see Fig. 4.1a around 460 MHz and 880 MHz).

It can be noted that there are cases where differences are negative, which means that the measured field was stronger than the predicted field. This occurred only in the

FM band, and might be attributed to: a) changes in the radiating source such as the power radiated or radiation pattern and b) propagation factors such as additive multiple reflections or a modal (resonant) response of the site being measured.

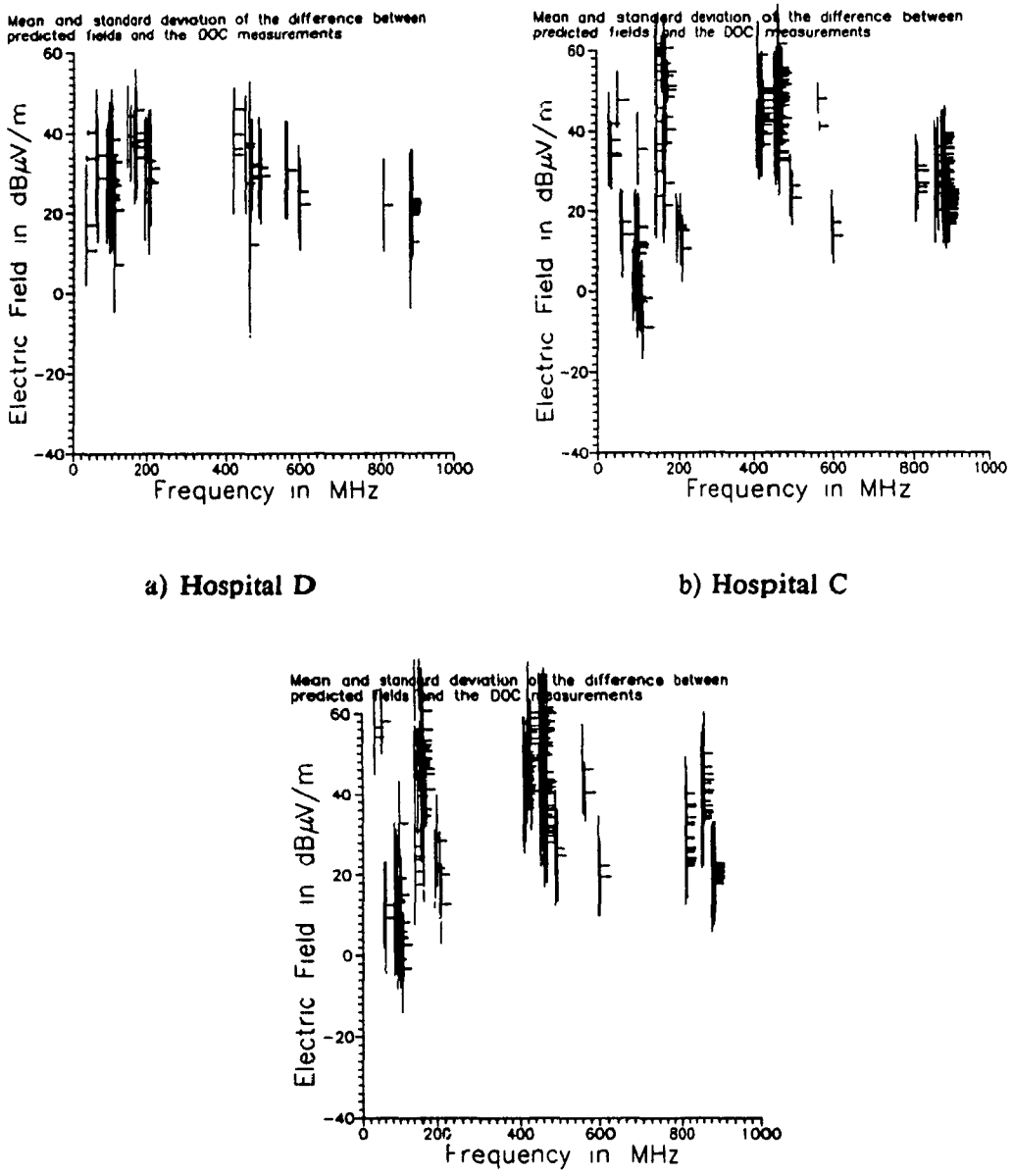

a) Hospital D

b) Hospital C

c) Hospital A

Figure 4.1 Difference between predicted and measured electric fields

The single most important conclusion one can draw from Fig. 4.1 is that the free space propagation model is not an adequate tool for predicting field strength levels in an urban environment. It does serve however to establish a reference baseline of the level of E.M. activity. Comparisons of the predicted fields to the measurements performed outside the hospitals show the even when broadcast transmitters enjoy a line of sight to the measurement site, as was the case for hospitals A and C, there is still a 20 dB difference between the measured and the predicted fields. When the broadcast transmitters do not have a line of sight to the measurement site, as was the case for hospital D (situation typical of an urban environment) this difference increases to 30 dB.

Despite the obvious inadequacies of the simple free space propagation model, it does nonetheless serve a useful purpose, especially as a consequence of these measurements:

a) as is common in propagation predictions, the free space model is important to establish a reference datum for other predictions or for the measurements.

b) the predictions do indicate the relative importance of each contributing radiating source.

c) the experience of the measurements provides an approximate predictive guideline for derating the calculated predictions. This guideline is that for line of sight cases the actual field will be of the order of 20 dB less and 30 dB less for shadowed cases, for urban situations comparable to those studied here.

4.3 Differences between standard and BOTES measurements

This section deals with the comparison between the two methods of measurements. Figure 4.2 is the same type of graph as the ones presented in the previous section. It shows the mean and standard deviation of the difference between standard measurements and BOTES measurements ($E_{BOTES} - E_{standard}$) for the entire set of measurements. Figure 4.3 presents the same data in another way: the E field measured by BOTES method is

plotted as a function of the corresponding E field obtained with the standard method. Most points lie between the two dashed lines, which indicate the location variability as reported in [7]. The full line in Fig. 4.3 represents the ideal relationship between the two sets of points: if the two measurement systems consistently obtained the same results at each survey site, all the points would align on a straight line of unity slope. Figure 4.4 a) is a frequency distribution of the mean of the distance between a point in Fig. 4.3 and the line of unity slope. It shows that the two measurement systems obtained results that were on average less than 5 dB apart. In the case of the FM band (around 100MHz), these differences were fairly negligible. Similarly, Fig. 4.4 b) is a frequency distribution of the standard deviation of the distance from a point in Fig. 4.3 to the line of unity slope. It shows that the variability between the results of the two systems is mostly below 10 dB, which is in accordance with the standard deviation of the location variability in urban areas reported in Skomal and Smith [8].

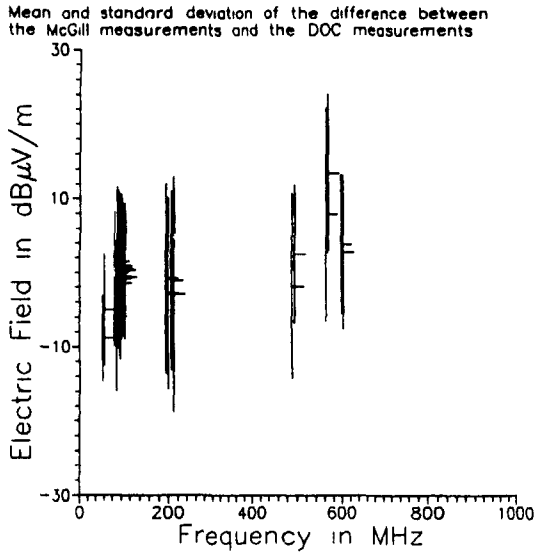

Figure 4.2 Difference between the BOTES and the standard measurements

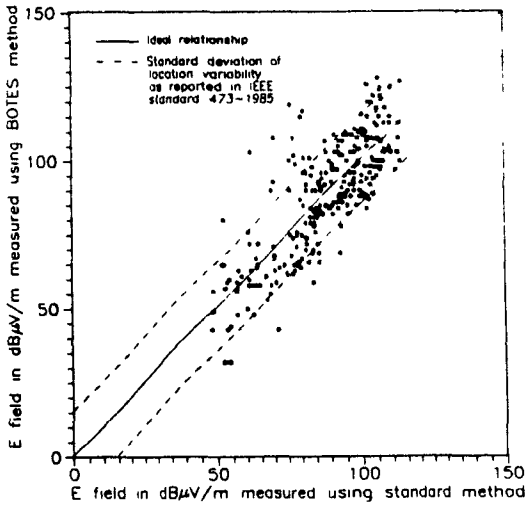

Figure 4.3 Comparison between standard and BOTES measurements

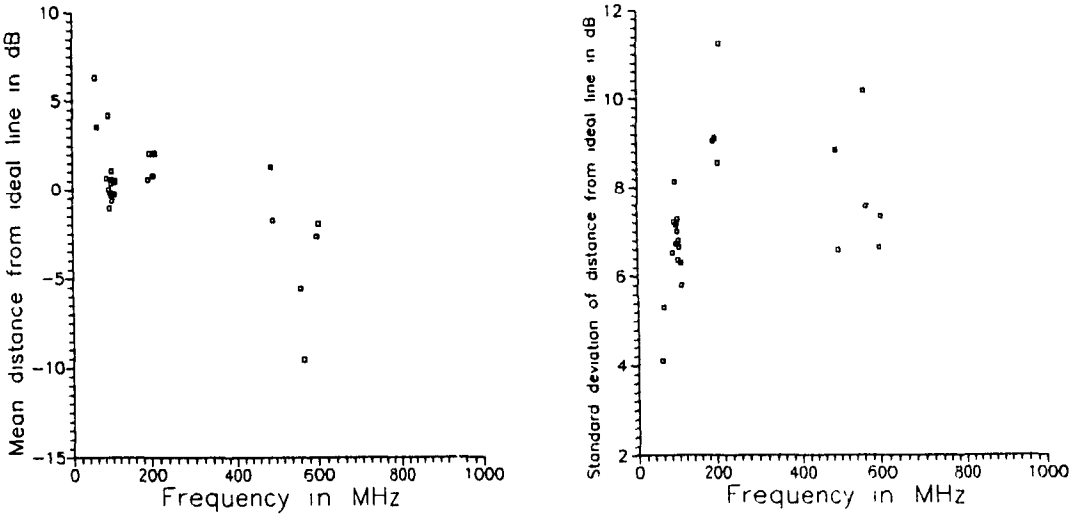

a) Mean

b) Standard deviation

Figure 4.4 Mean and standard deviation of scatter from ideal line as a function of frequency (7 TV stations and 10 FM radio stations)

The deviation from the ideal line may be attributed to spatial and temporal distributions, and to the theoretical (rather than empirical) calibration of the probe. That

the results of the two methods be different when the antennas are not located in the same physical space is expected, since the spatial variations of the E and H field vectors inside any structure are due to multiply interfering waves. Here, this effect is further enhanced by the complexity of the structure under study, which consists of two metallic grids (floor and ceiling) covered by a dielectric (concrete), between which a variety of sizeable metallic objects are strewn (beds, lockers, filing cabinets, support columns). To illustrate the complexity of the shape of the fields indoors, Fig. 4.5 shows the spatial distribution of the E field in the lobby of a building in downtown Montreal.

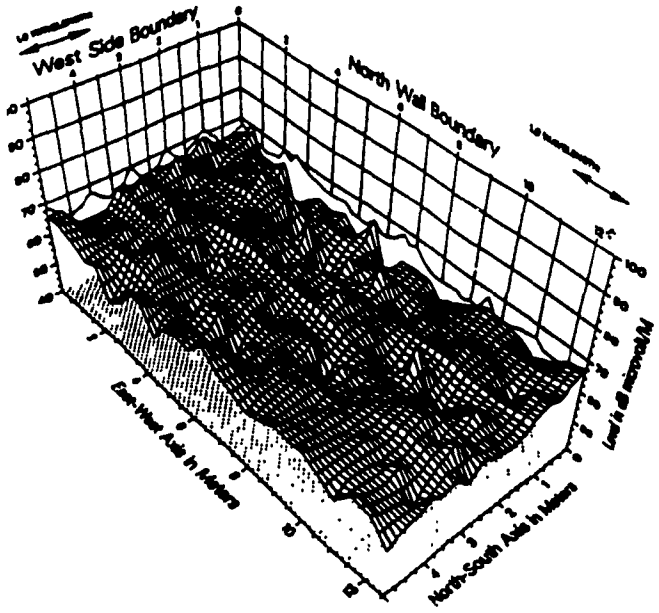

Figure 4.5 Field distribution in a building
(as measured by LeBel and plotted by Banik [12])

To alleviate the problem of field distribution, the measurements could be taken in exactly the same point. The easiest point to find is the absolute maximum, and both measurements could be taken at whatever point they find to be absolute maximum. However, a comprehensive, three dimensional survey of every room would be needed to find that point. Fortunately, this point is likely to be near the opening facing the broadcast tower (see Fig. 4.6).

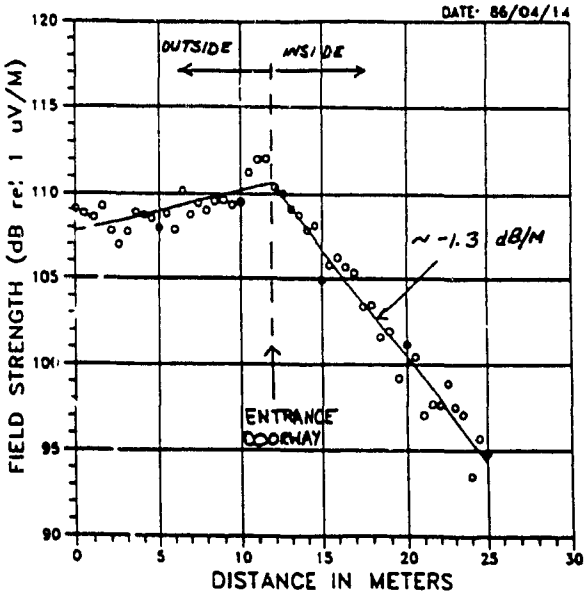

Figure 4.6 Intensity of fields inside and outside a building
(as measured by LeBel and plotted by Banik [17])

Even if the point of absolute maximum is used for both measurements, the resulting spectra are not going to be identical, because of the two different antennas. The BOTES probe is roughly the size of a fist, whereas the standard antenna was about the size of a torso. It can be expected that the output of the large biconical antenna would be an average of the smaller probe's output over the same volume. Therefore it makes sense to compare the measurements on the average rather than on a point by point basis, where differences of as much as 40 dB have been encountered.

Even if the same equipment were used to record the same signal at two different times at the same point, two different spectra would result, because of the temporal variations of the signals. This can be caused by changes in the intervening propagation path, by changing modulation levels and similar causes. A simple experiment was performed in downtown Montreal: the maxima and minima of the signals of all the stations in the FM band were recorded over a one hour period at a particular point in

one specific location. The typical difference between maxima and minima was 30 dB. This experiment demonstrated dramatically that there are major temporal variations in broadcast signals, variations that affect a measurement's repeatability.

The idea behind making parallel measurements was to obtain an empirical calibration curve for the BOTES probe based on industrial standard techniques used by DoC. Even though the above-mentioned variations can be averaged out if enough surveys are performed, an empirical curve could not be obtained from this set of measurements. Because some broadcast signals were very low and because of the insensitivity of the BOTES probe, a number of the signals were below the spectrum analyzer's noise floor. In these instances, the signal was recorded as being at noise level and the analysis was performed as for any other signal. This saturation led to artificially high McGill signals in comparison with DoC's. Saturation is the sole reason behind the large difference between the two measurements of channel 29 which operates at approximately 560 MHz (see Fig. 4.4a).

4.4 Differences between "good" rooms and "bad" rooms

One of the main goals of the pilot project was to develop the means to predict areas where medical devices are likely to malfunction due to EMI (i.e. "bad" rooms) and areas where devices are likely to work properly (i.e. "good" rooms). It was originally thought that this could be done simply by measuring the environment but, as shown in chapter 3, none of the sites surveyed had an ambient EME worse than that prescribed in FDA-MDS-201-0004 (1979). Therefore, none of the medical equipment should have been the victim to EMI in any of the rooms surveyed, had it conformed to the standard. Unfortunately, since the standard has not been adopted by all medical equipment manufacturers, and because medical equipment purchasers do not require compliance with this standard, some medical devices have malfunctioned due to EMI in a number of the rooms surveyed.

In fact, one device, a radiant heater for newborns, malfunctioned while the measurements were being made in one of the survey sites. The radiant heater monitored the skin temperature of the premature baby with a temperature probe, the output of which was compared to a reference level such that a baby would be warmed by an infrared heater whenever the temperature would fall below the reference. However, it was discovered that the baby's temperature reading could be changed just by walking around the instrument, thereby altering the interference pattern of the ambient fields. Subsequent tests have shown that the device malfunctioned when subjected to emissions in different bands (VHF, UHF and cellular), thereby demonstrating the broadband characteristics of the failure mechanism. A demonstration of the malfunction was taped on videocassette for visual documentary evidence.

Therefore, a number of factors other than the electromagnetic environment come into play:

a) **The type of signal to which a device must respond.** Devices designed to react to weak signals are necessarily sensitive, therefore their immunity level is lower. Correspondingly, devices designed to respond to signals with significant high frequency content risk accepting components of the ambient EME as well as the intended signals.

b) **The design of the device.** If the front end of the instrument rectifies the input signal, it will demodulate ambient RF signals, producing significant low frequency components. Similarly, if the front end does not sufficiently block out higher frequency components, these could interfere with the proper processing of the information. This is discussed further in chapter 5.

c) **Age and the way the equipment was maintained.** The hospital is a harsh environment for electronic equipment. Aside from the inevitable physical punishment, these devices are cleaned with powerful disinfectants that might chemically affect the components, the soldering joints or the PCB substrates, thus resulting in possible non-linear conductive paths.

All these additional factors play important roles in determining whether or not a device will malfunction.

Nonetheless, in regards to the determination of the electromagnetic environment in which a malfunction may occur, malfunctions were observed in environments where the EEF in the FM band exceeds 110 dBμV/m. To solve the problem when a malfunction occurred, either the machine was repaired, "hardened" when a clear causal relationship could be established or it was moved out of harm's way to a location where the EEF in the FM band was about 15 dB lower, thus providing rough definitions of "good" and "bad" rooms: the EEF in the FM band was 110 dBμV/m or more in "bad" rooms, while it was 95 dBμV/m or less in "good" rooms.

The only reliable technique for determining the average ambient E.M. environment which causes malfunctions would entail the determination of the susceptibility characteristics of many malfunctioning devices. This will be a necessary, but time and equipment consuming, task which will require a major study of the failure modes of equipment. The next chapter is a preliminary examination of some aspects of such a study.

Chapter 5 SIMULATION

5.1 General

This chapter provides an estimate of the possible effects produced in typical biomedical equipment by the ambient E.M. field levels presented in chapter 3. A straightforward analysis follows to establish whether the order of magnitude of the fields encountered can induce unwanted signals comparable to the signal levels at which the equipment would normally operate. For this reason, the modelling used, especially that of the coupling mechanism (the effective antenna), is not a detailed rigorous one, but rather an idealized form with the emphasis on the broad spectral response of the electrode wire. This then makes it possible to use the measured spectral distributions to assess the global response of the equipment.

The EME in health care facilities having been defined through simulation and measurement, the next logical step in the analysis of the EMI problem in hospitals involves considering the effect of the ambient EME on medical devices. This chapter simulates the effect of three typical spectral distributions (one from each hospital A, C and D) on diagnostic devices operating in the 100 kHz range. Since a growing proportion of instruments now use digital technology for processing the data, only the front end of such a device will be investigated. In any case as in any signal processing system, it is the high sensitivity first stage which is most sensitive to unwanted noise or disturbing signals.

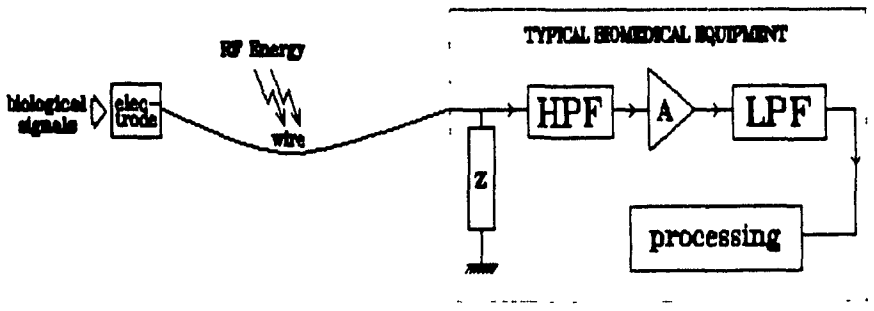

Figure 5.1 Schema of the EMI situation in hospitals

Figure 5.1 represents the arrangement for monitoring the vital signs of a patient lying on a large metallic bed. An electrode on the patient's body senses the electrical biological or diagnostic signals and transmits them via an unshielded wire to the medical device. In this particular case, the signal is high pass filtered (HPF) to remove the 60 Hz noise, then it is amplified (A) and filtered again (Low Pass Filter) to eliminate the higher frequency components. The signal is then ready for digital, or other, processing.

5.2 General assumptions

Ambient E fields will be assumed constant over the length of the electrode wire. This is partially justifiable, since the spectra used are those obtained by the DoC with an antenna roughly the same length as such a wire, and therefore the electric fields used actually represent an average of the E fields over the length of such a wire. The conductor is assumed to be perfectly conducting, uninsulated, straight and parallel to the fields. The electromagnetic effects of nearby conducting bodies, such as the chassis of the instrument, the body of the patient and the metallic bed are not considered in this estimate.

Compared to the signals measured in chapter 3, electrical biological and diagnostic signals are usually slow and weak. Typical spectral contents are in the Hertz to the low MegaHertz range and amplitudes generally are in the microvolt to millivolt range. If the processing is performed digitally, as is becoming more and more common, the amplifier stage must provide enough gain to bring the signal to TTL levels of 5 volts to allow conversion to digital form. This requires gains of 5 000 to 5 000 000 over the frequency band of interest, values that are easily obtainable with current commercially available operational amplifier circuits. The frequency response of these op-amps will roll off with 15 dB per decade beyond the cutoff frequency, thus forming a part of the low pass filter. In addition, the low pass filter itself will provide at least 10 additional deciBels of attenuation per decade, but a more probable estimate would be 20 to 30 dB/decade.

The amplifier and all components of the front end of the instrument are considered linear and the frequency dependance of the other components will be neglected.

5.3 Coupling to the wire

With these numbers in mind, the simulation can now proceed. Since it is bare, the wire will be analyzed as if it were one half of a dipole of length L. Starting from the equation for the effective length (h_e) of a dipole found in [13],

$$h_e = \frac{1}{I_o}\int_0^{\frac{L}{2}} I(z)dz$$

substituting with the theoretical current distribution on a dipole,

$$I(z) = \sin\left[\frac{2\pi}{\lambda}\left(\frac{L}{2} - |z|\right)\right]$$

and integration yields a compact expression for the theoretical effective length of a dipole:

$$h(L,\lambda) = \frac{L}{\max\left[\sin\frac{2\pi}{\lambda}\left(\frac{L}{2} - y\right)\right]_{0\le y\le\frac{L}{2}}}\frac{2\lambda}{\pi}\sin^2\left(\frac{\pi L}{2\lambda}\right)$$

The voltage induced on the dipole by the field E can be expressed as

$$V(\lambda) = h(L,\lambda)E(\lambda)$$

where $E(\lambda)$ is the measured spectral distribution. For example, the effective length (or transfer function relative to 1 meter) of a 1.5 meter wire is presented in Fig. 5.2, where it is clear that while the wire acts as a comb filter with cutoffs at

$$f = \frac{2nc}{L} = n \times 200\,MHz$$

and it has some relative gain in the region of the FM band, at about 100 MHz.

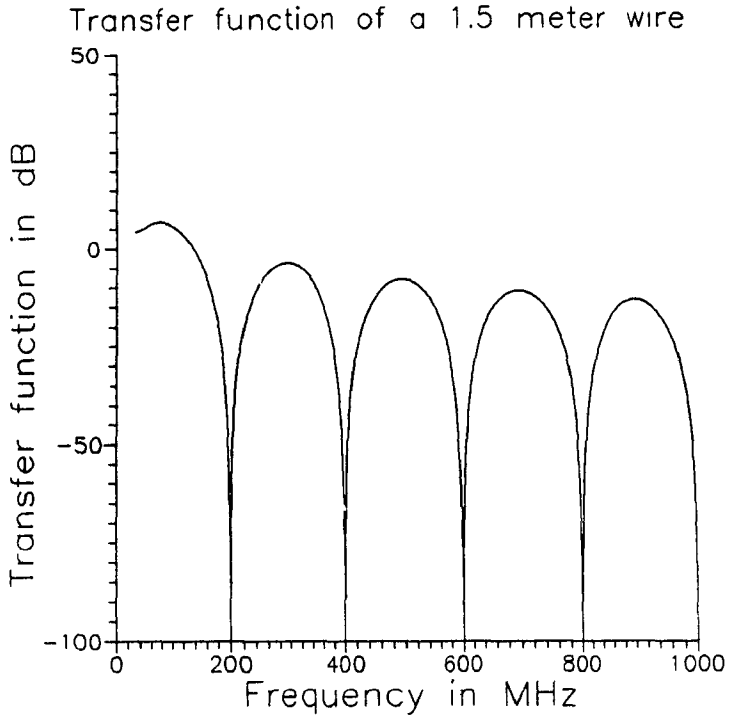

Figure 5.2 Effective length (or transfer function) of a 1.5 meter wire as a function of frequency

The voltages induced on a wire are the subject of Fig. 5.3. These graphs show, for each of three locations, the response of the wire whose transfer function is shown in fig. 5.2 to the measured spectral distributions of each of the three locations. The filtering action of the wire can be seen to have an obvious effect on the spectrum. It is worth noticing however that the amplitude of the FM band, which is approximately 105-110 dBμV or 200 mV, is in or above the range of amplitudes of the biological and diagnostic signals. If unattenuated, this unwanted signal might saturate the amplifier and thus significantly alter the shape of the measured biological or diagnostic signal. However, nonlinearities are not considered in the present work.

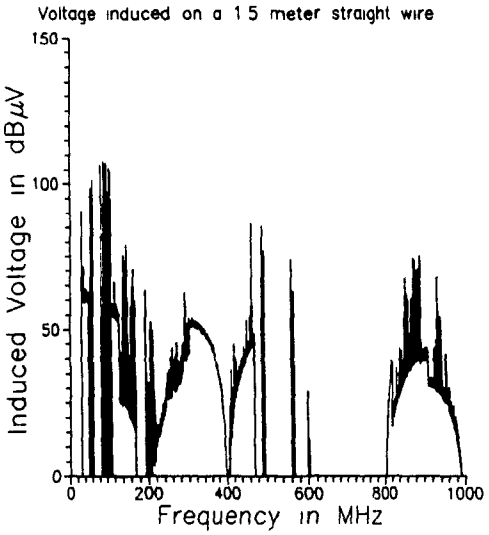

a) Hospital D

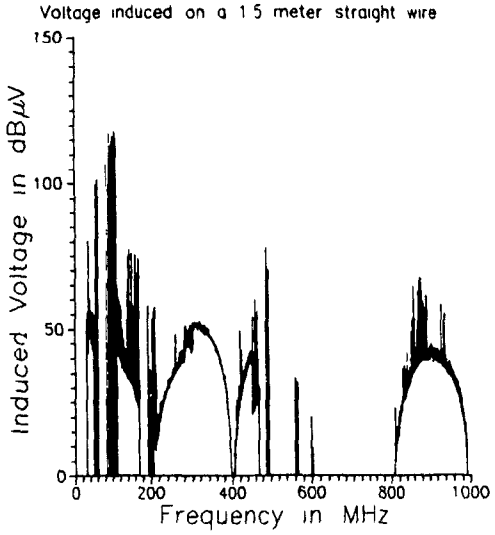

b) Hospital C

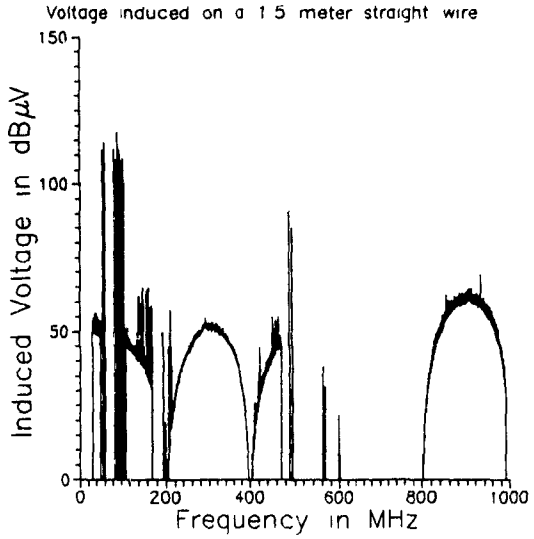

c) Hospital A

Figure 5.3 Voltages induced on a 1.5 meter wire

(for comparison with measured EME, see Fig. 3.1)

5.4 Progressive processing of the spectrum by the biomedical device

The high pass filter will not have any effect on the shape of the distribution of Fig. 5.3 since this filter eliminates 60 Hz noise but passes the biological and diagnostic signals. The low pass characteristics of the amplifier and the low pass filter can be combined into one, since both cutoff frequencies will likely be equal to or higher than the highest frequency component of the biological or diagnostic signal. Therefore in the analysis, the amplifier and low pass filter were combined into one block having 2×10^5 (105 dB) gain and an attenuation of 35 dB/decade starting at a cutoff frequency of 100 kHz. The shape of the resulting spectrum is shown in Fig. 5.4. It should be noticed that the lower frequency components of the distribution are unchanged from Fig. 5.3, because the gain of the amplifier offsets the attenuation of the filters. On the other hand, the upper frequency part of the spectrum has decreased significantly.

At this stage of the device, the biological and diagnostic signals have an amplitude of approximately 5 volts or 135 dBμV, which is only 8 dB above the strongest peaks of the signal in Fig. 5.4, and there are a number of signals around 122 dBμV or 1.25 volts. On its own, any peak above 114 dBμV or .5 volt could be considered disruptive. But, even when the spectral distribution does not rise above 110 dBμV, as in Fig. 5.4 a), the composite effect that the distribution may have in the time domain must be examined. The spectral distributions of Fig. 5.4 could be regarded as frequency representations of time signals that can be obtained by inverse fourier transform. Such a transformation has been done and the results are presented in Fig. 5.5, showing the nature of the interfering signal in the time domain.

While it is doubtful that the signals in Fig. 5.5 contain enough energy to damage integrated circuits in the biomedical device, their amplitudes are nevertheless high enough to alter the output of an analog to digital converter or to disrupt a control circuit. A disrupted control circuit was the cause behind at least one reported malfunction attributable to EMI.

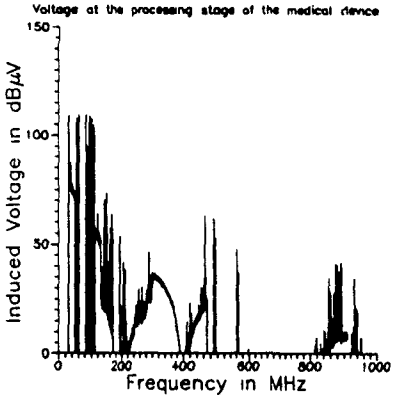

a) Hospital D

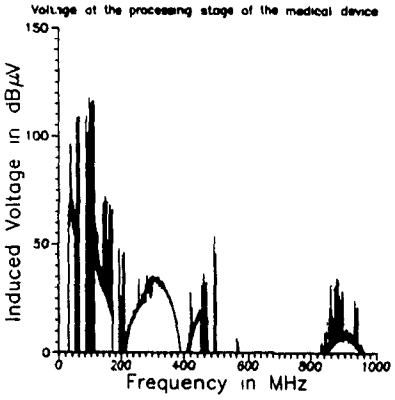

b) Hospital C

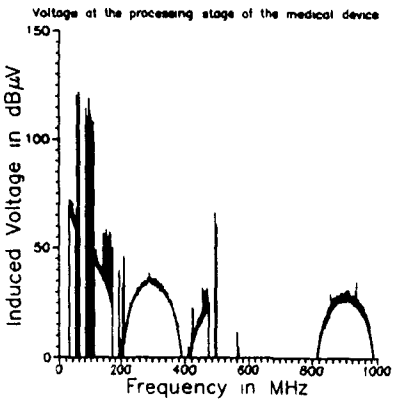

c) Hospital A

Figure 5.4 Frequency domain

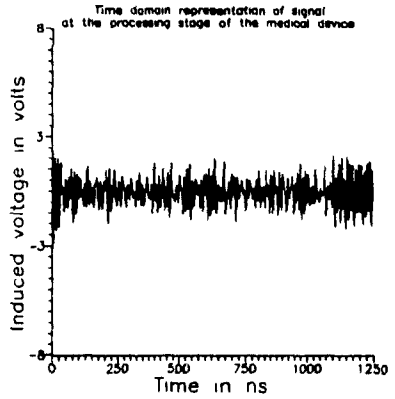

a) Hospital D

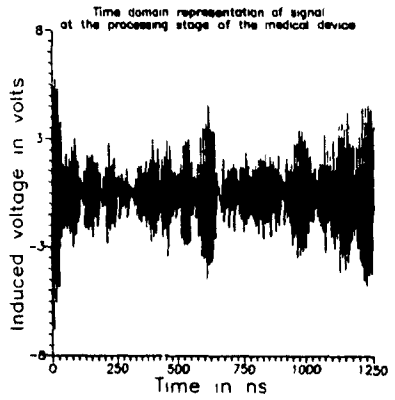

b) Hospital C

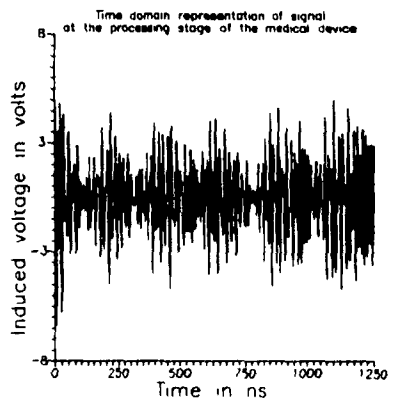

c) Hospital A

Figure 5.5 Time domain

Representations of the signals at the processing stage of the device

Figure 5.6 shows the result of the addition of the noise of Fig. 5.5 to a 5 volt, 100 kHz cosine wave representing a biological or diagnostic signal. In all three cases, the noise varies much more rapidly than the main signal, but in 5.6 c), the noise exhibits a beat that might introduce artifacts in the processed signal. The most serious disruptions occurs for cases b) and c), where a weaker biological or diagnostic signal might be completely masked.

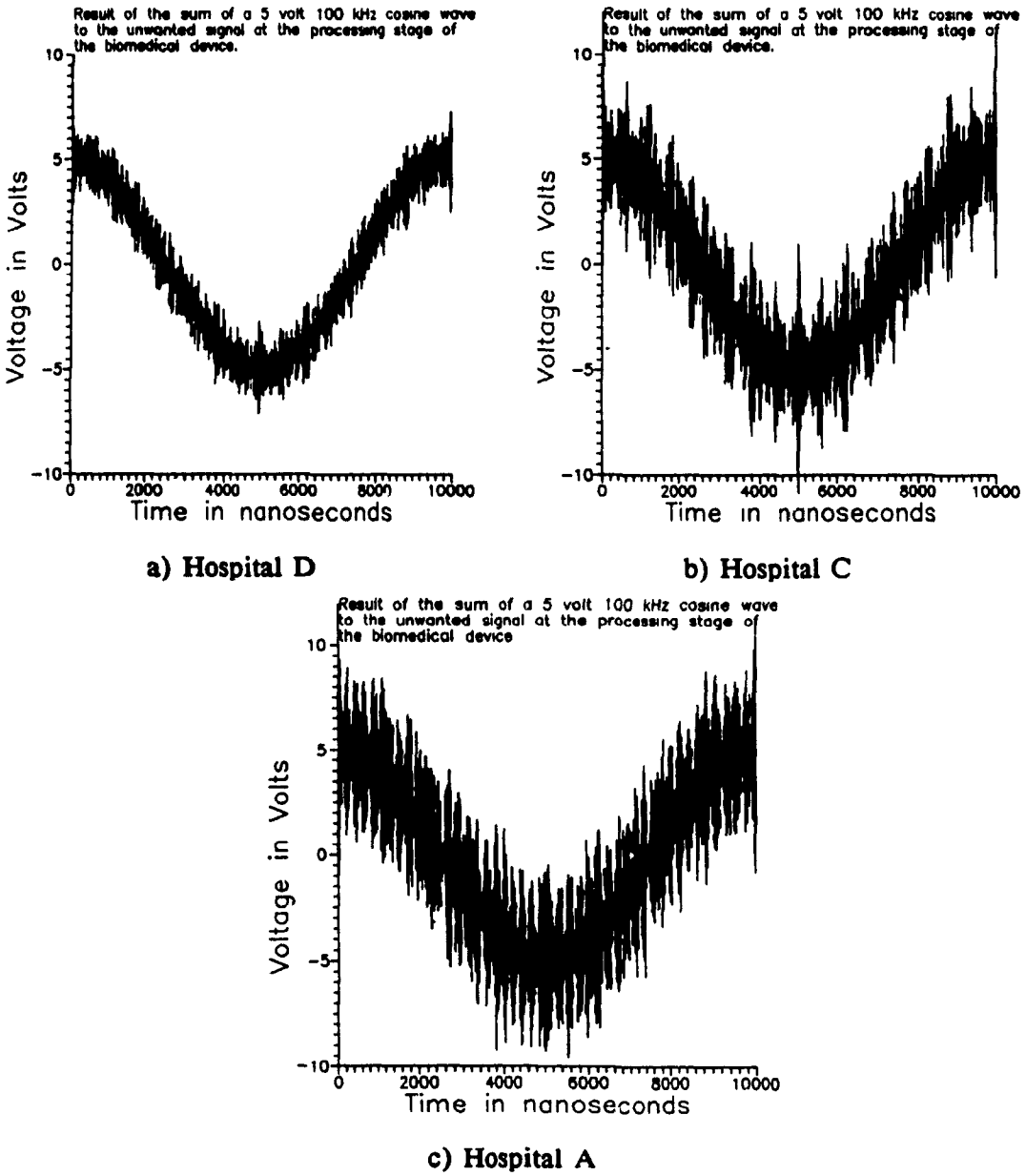

a) Hospital D

b) Hospital C

c) Hospital A

Figure 5.6 Noisy biological or diagnostic signal at the processing stage of the biomedical instrument

The intent of this chapter was not to provide a exhaustive and in depth analysis of the equipment failure mode problem, but rather to outline a method which might be followed in greater detail in order to seek a remedy to a failure of this nature. Nonetheless, it has been shown that high field strengths can disrupt the normal processing of biological and diagnostic signals, even when the inherent non-linearities of a biomedical device are not considered.

As suggested above, a major research effort is required to study the failure mode problem in general and in particular to examine the non-linear problem. Thus, as a first step in such a study, it would be appropriate to consider the effect of a rectifying diode at the output of the probe wire, as a first stage of the medical device.

In addition to the theoretical simulation, an in-depth study of the failure mechanism will require laboratory investigations involving a simulation of the E.M. environment in order to determine equipment failure modes. Such laboratory simulation is known to form part of a major research program at the University of Toronto, which is oriented to examining the effect of EMI on telecommunication equipment.

Chapter 6 CONCLUSION

The primary objective of this thesis was to determine the ambient EME in metropolitan hospitals, in order to assess the degree to which such an environment is a threat to biomedical equipment. This also gave the opportunity to compare different measuring techniques. In addition, the results allowed a preliminary simulation of the effects that the kind of EME measured in this study might have on a potential victim.

This chapter highlights the observations and conclusions already enumerated in previous chapters and also proposes recommendations for further studies of the problem. As recommended in the guidelines for master's theses, claims of originality are indicated in boldface.

For this pilot study, E field levels were calculated for every floor of three major hospitals in the Montreal area. These predictions were acceptable for predicting the harshness of the EME and the overall shape of the spectral distribution, but proved unreliable for absolute values because of the complexity of the propagation problem in metropolitan areas. A more refined propagation model should be sought for more precise predictions, one that would take into consideration the effects of other buildings as well as those due to the building under study. The development of such a model might make use of the 20 and 30 dB differences that were noted between free space predictions and measurements for line of sight and shadowed locations.

Subsequently, electric fields were measured in a total of 21 sites in the three hospitals. Field strengths generally ranged from 105 to 125 dBμV/m, but levels as high as 135 dBμV/m have been recorded. At the other end of the scale, the lowest signals were observed in a room partially shielded by a metallic vapor barrier. This prompts the suggestion that metallic vapor barriers be used in new hospital construction, instead of plastic sheeting. On a smaller scale, field strengths were noticeably lower behind the screened portion of a window than behind the unscreened part. This also prompts the suggestion that, in some cases, relatively simple structural alterations may reduce the potential hazard to acceptable levels.

None of the spectral distributions ever rose above the susceptibility limits prescribed by the Food and Drug Administration standard on EMC for medical devices. Therefore, seeing that some devices did malfunction due to EMI in the rooms that have been surveyed, this indicates that they probably did not comply with the standard. **This prompts the suggestion that the legal status of the FDA standard for EMC for medical devices be changed from an unregulated voluntary recommended practice to a fully regulated mandatory standard.** In addition, those procuring such equipment should insist on compliance with the standard at the time of purchase and thereafter during use.

Since some frequency bands are more cluttered than others, the Equivalent Electric Field (EEF) was used to estimate the power content in a given frequency band. High EEF in the FM band was characteristically common to rooms where there had been malfunctions. The EEF in the rooms to which previously malfunctioning devices were moved and then subsequently functioned properly was found to be 15 dB lower than in the locations where they malfunctioned.

A novel measurement technique used in this study was based on the philosophy of an innovative E field probe. Since the structure of the fields inside a room, roughly the size of the median wavelength to be measured, is very complex, a representative measurement must consider the following:

- the measuring equipment must be small compared to the room and to the objects in the room. Ideally, it should also be small compared to the shortest wavelength to be measured.
- since the field structure is a complex interference pattern, the E field vector is best characterized by measuring its three orthogonal components and summing them vectorially.
- the sensitivity of the measuring equipment need not be better than 75 dBμV/m since only high level fields are of interest. The equipment associated with the probe may thus be simpler and less expensive.

To this end, **a small three polarization, omnidirectional, broadband, electrically small BOTES E field probe was designed and built.** The results obtained with it were necessarily different from those obtained with the standard technique because of the spatial and temporal distributions associated with the E field vector, but on the average they produced comparable results (the average difference was less than .1 dB, with a standard deviation less than 8 dB).

Lastly, the spectral distributions obtained by measurement were used to simulate the effects a typical EME might have on a medical device. It was found that high field strengths, especially those in the lower part of the spectrum, can couple to a biomedical device through an electrode wire and disrupt the normal processing of biological and diagnostic electric signals. However, this type of analysis of the failure mode of potential victim equipment merits an extensive separate study. Nevertheless, the results of the measurements of the present study provide essential input information for the failure mode analysis.

This study represents a preliminary examination of a complex problem. In order to obtain a more complete assessment of the general situation, more hospitals must be surveyed, and field structures inside the hospitals determined in detail. Further surveys should include a larger number of sites, more samples per site and they should cover a wider frequency span more completely. For example, lower frequencies, which are potentially more harmful to medical devices, should be included, and presently unused portions of the spectrum need to be tested from a propagation and victim point of view. The contribution of the DND to the latter point was crucial in this experiment, but further, more intense involvement would be desirable. In addition, further studies should be followed by an examination of impulsive and commuted signals, whose sources could be either from inside or outside the hospital. Finally, a better understanding of the spatial and temporal distributions of the E fields might shed some light on the meaning to be given to measurements.

Appendix A DESIGN OF A BROADBAND, OMNIDIRECTIONAL, TRIAXIAL, ELECTRICALLY SMALL (BOTES) ELECTRIC FIELD PROBE

A.1 General

To enable the McGill Biomedical Engineering Group on EMC to make preliminary surveys in potentially troublesome areas on a continuing basis, the design of an appropriate receiving antenna was called for. The requirements were the following:

- the sensing probe should be small because of the typical lack of space in hospitals and so as not to interfere with the field structure.
- the probe should handle moderately high field strengths (130 dBμV/m)
- the antenna should have good working characteristics over the entire band of interest, 10 to 1000 MHz.
- finally, the probe should be isotropic and sense an E-field regardless of its polarization.

After a preliminary study of biconical, spherical and parallel plate dipoles, it was found that the only design which met all the above criteria was one involving the measurement of all three polarizations with three orthogonal, electrically small dipoles.

A.2 Electrical behavior

In order to remain electrically short over the band of interest, the length of the dipole should not exceed one tenth of the shortest wavelength. In this case, the highest frequency is 1 GHz, which corresponds to a 30 cm wavelength. Thus the dipole should be shorter than 3 cm. On the other hand, the voltage at the terminals of an electrically small antenna is given by

$$V = hE$$

where h is the physical length of the dipole and E is the component of the electric field parallel to the antenna. Since V should be maximized for a given E, h should be as large as possible. By combining this latter requirement with the former, the compromise conclusion is that each of the three dipoles should be 3 cm long.

A.2.1 Calculation of impedance

The impedance of an electrically small dipole is easily calculated using the open ended transmission line approximation. Then

$$Z(l) = Z_0\left(\frac{Z_L\cos\beta l + jZ_0\sin\beta l}{Z_0\cos\beta l + jZ_L\sin\beta l}\right)$$

where $Z_L = \infty$ since the line is open and the characteristic impedance of the line Z_0 = 100Ω. Therefore

$$Z(l) = Z_0\frac{\cos\beta l}{j\sin\beta l} = -jZ_0\frac{\cos\beta l}{\sin\beta l} \approx -j\frac{Z_0}{\beta l} = -j\frac{100}{\beta l}$$

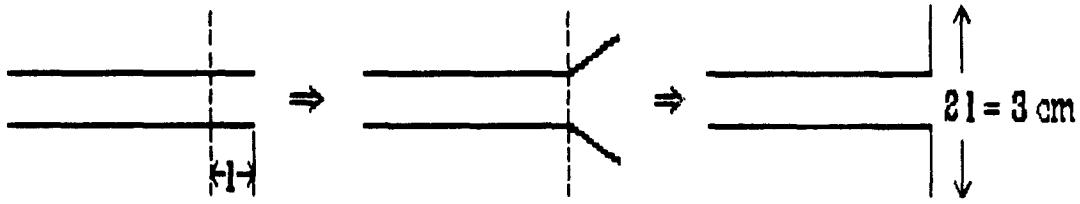

Figure A.1 Open ended transmission line approximation

Since by Fig. A.1 l = .015 meter

$$\beta l = \frac{2\pi l}{\lambda} \le \frac{\pi}{10}$$

so that

$$Z_a = Z(l) = -j\frac{100c\,1}{2\pi l\,f} = -j\frac{10^{-12}}{\pi f}$$

The impedance is plotted as a function of frequency in Fig. A.2.

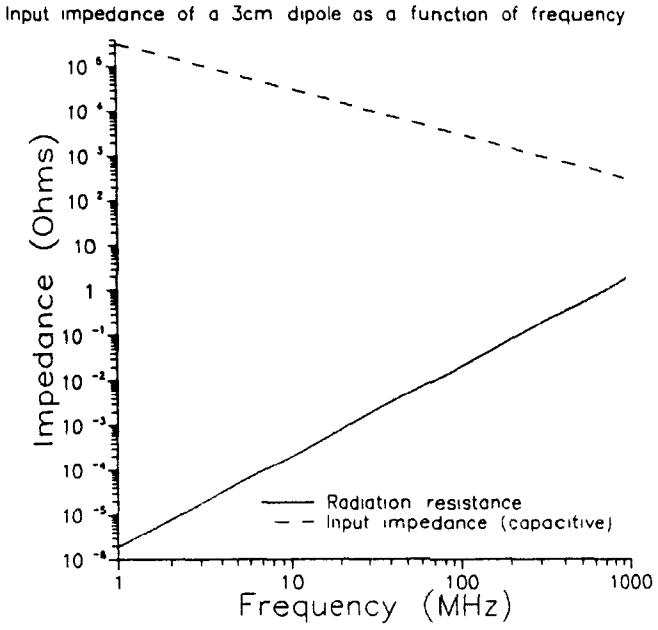

Figure A.2 Impedance of a 3 cm dipole as a function of frequency

A.2.2 Calculation of the antenna factor

The antenna factor is readily calculated given the circuit representation of Fig. A.3 where V_E is the voltage generated at the terminals of the dipole, Z_a is the impedance of the antenna, R_L is the load impedance and V_0 is the voltage measured at the input of the measuring device e.g. spectrum analyzer. From the previous equations,

$$V_E = hE$$

where h = .3 meter, and from Fig. A.3,

$$V_0 = \frac{V_E R_L}{R_L + Z_a} = \frac{hE R_L}{R_L + Z_a}$$

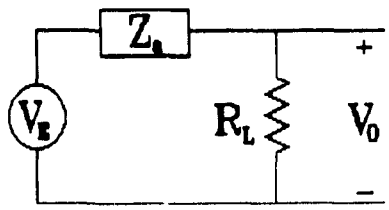

Figure A.3 Circuit representation of antenna

such that

$$\frac{V_0}{E} = \frac{hR_L}{R_L + Z_a}$$

For this experiment, $R_L = 100\Omega$ and $Z_a = \frac{-j10^{12}}{\pi f}$. Therefore

$$\frac{V_0}{E} = \frac{.03 \times 100}{100 - \frac{j10^{12}}{\pi f}}$$

$$\left|\frac{V_0}{E}\right| = \frac{3}{\sqrt{10^4 + \frac{10^{24}}{\pi^2 f^2}}}$$

but since $f_{max} = 1$ GHz, $f_{max}^2 = 10^{18}$ Hz^2 and $\frac{10^{24}}{\pi^2 f_{max}^2} \gg 10^4$

then the transfer function can be approximated as

$$\left|\frac{V_0}{E}\right| \approx \frac{3}{\frac{10^{12}}{\pi f}} = \frac{3\pi f}{10^{12}}$$

In logarithmic form,

$$\left|\frac{V_0}{E}\right|(dB) = 20\log\left(\frac{3\pi f}{10^{12}}\right) = 20\log f - 220.5$$

the graph of which is presented in Fig. A.4

Even though the antenna factor is determinedly negative (attenuating), the high field strengths predicted in Chapter 2 still yield measurable signals, given the equation

Expected E field in dBμV/m + AF in dB = signal in dBμV

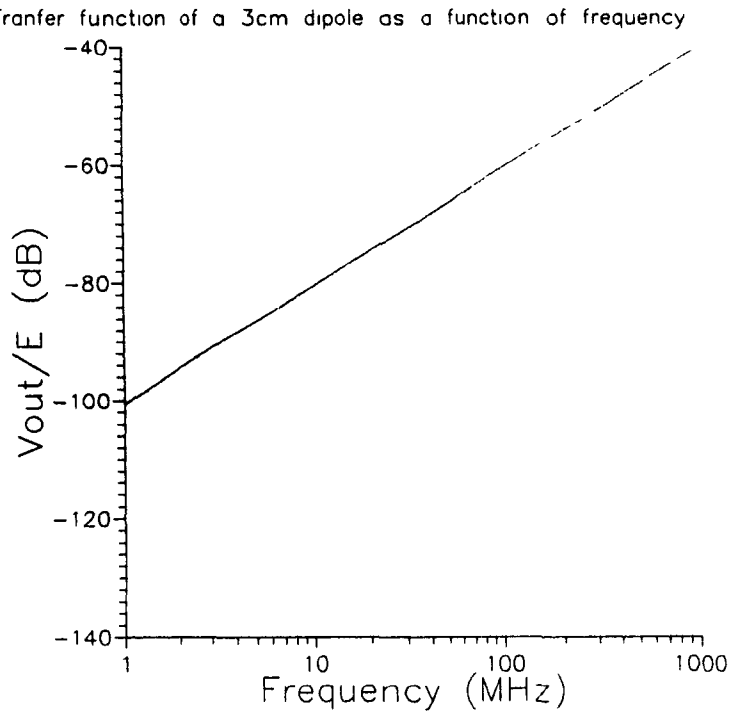

Figure A.4 Antenna factor of a 3 cm dipole as a function of frequency.

For the frequency range of interest, the antenna factor is never less than -80 dB and the predicted E field levels are higher than 80 dBμV/m which yield signals stronger than 0 dbμV. Assuming that the typical noise floor of a portable spectrum analyzer is at -107 dBm or 0 dbμV, the signals would be detectable.

A.3 Feeding arrangement

The three short dipoles were disposed in a novel way while maintaining orthogonality. Instead of having the centers of the dipoles meet in a common point as is usually the case, the dipoles were disposed around an imaginary circle, much like the National Bureau of Standards design of a BIRES [9].

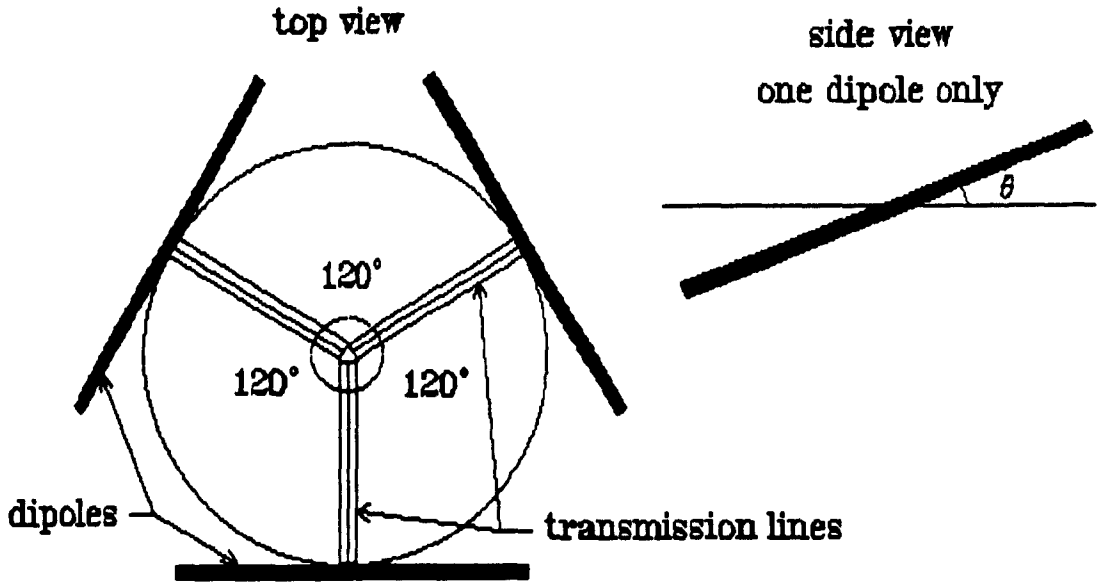

Figure A.5 Feeding arrangement of E field probe

The angle Θ that each dipole must make with the horizontal is calculated by insuring that the cross products of any two vectors give the third, assuming that they have a unit length. From the top view of Fig. A.5, the coordinates of the projection of the vectors on the x-y plane can be found. They are:

element 1 : projection length x $(\hat{j})$

element 2 : projection length x $(-\sqrt{\frac{3}{2}}\hat{i}-\frac{1}{2}\hat{j})$

element 3 : projection length x $(\sqrt{\frac{3}{2}}\hat{i}-\frac{1}{2}\hat{j})$

From Fig. A.6 where the vector has unit length, one finds that the projection length is none other than cos Θ, and that the length of the vector along the Z axis is sin Θ.

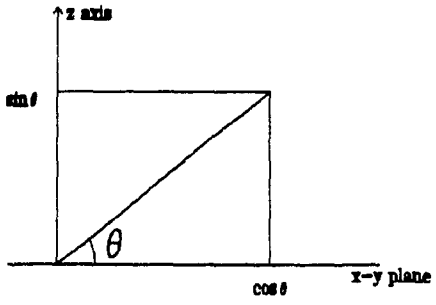

Figure A.6 Side view

Therefore the coordinates for each element are:

element 1 : $\cos\theta\hat{j} + \sin\theta\hat{k}$

element 2 : $-\sqrt{\frac{3}{2}}\cos\theta\hat{i} - \frac{1}{2}\cos\theta\hat{j} + \sin\theta\hat{k}$

element 3 : $\sqrt{\frac{3}{2}}\cos\theta\hat{i} - \frac{1}{2}\cos\theta\hat{j} + \sin\theta\hat{k}$

Clearly each element has unity length, such that if all three vectors are orthogonal, the cross product of the first with the second should give the third, i.e.

element 1 x element 2 = element 3

element 2 x element 3 = element 1

element 3 x element 1 = element 2

Because there are three components to each equation, this is a set of nine equations with only one unknown, Θ. Fortunately, they all yield the same solution:

$$element\,1 \times element\,2 = \begin{vmatrix} \hat{i} & \hat{j} & \hat{k} \\ 0 & \cos\theta & \sin\theta \\ -\sqrt{\frac{3}{2}}\cos\theta & -\frac{1}{2}\cos\theta & \sin\theta \end{vmatrix} = -\frac{3}{2}\cos\theta\sin\theta\hat{i} - \sqrt{\frac{3}{2}}\cos\theta\sin\theta\hat{j} - \sqrt{\frac{3}{2}}\cos^2\theta\hat{k}$$

Equating term by term to element 3:

$$i: \frac{3}{2}\cos\theta\sin\theta = \sqrt{\frac{3}{2}}\cos\theta \Rightarrow \sin\theta = \frac{1}{\sqrt{3}}$$

$$j: -\sqrt{\frac{3}{2}}\cos\theta\sin\theta = -\frac{1}{2}\cos\theta \Rightarrow \sin\theta = \frac{1}{\sqrt{3}}$$

$$\hat{k}: \sqrt{\frac{3}{2}}\cos^2\theta = \sin\theta \Rightarrow \sqrt{\frac{3}{2}}(1 - \sin^2\theta) = \sin\theta$$

$$-\sqrt{\frac{3}{2}}\sin^2\theta - \sin\theta + \sqrt{\frac{3}{2}} = 0$$

and therefore

$$\sin\theta = \frac{1 \pm \sqrt{1 + 4\left(\frac{3}{4}\right)}}{-\sqrt{3}} = \frac{1 \pm 2}{-\sqrt{3}} = \frac{1}{\sqrt{3}}, -\sqrt{3}$$

only $\theta = \sin^{-1}\left(\frac{1}{\sqrt{3}}\right)$ is retained since θ is required to be real. Therefore if $\Theta = 35.26°$ then all three dipoles are orthogonal.

A.4 Balun

Most traditional balun configurations of a dipole feeding a coaxial line are either resonant or narrow band. Since a 20:1 bandwidth is required here, such an arrangement was not considered. Also, because the feeding arrangement does not leave enough room for a balun near each dipole's feed point, the balun problem was pushed further down the transmission line: each half of each dipole was actually the center conductor of its own 50 Ω semi-rigid coaxial cable. This is why the characteristic impedance of the line in the calculations of section A.2 was 100 Ω rather than the usual 50 Ω.

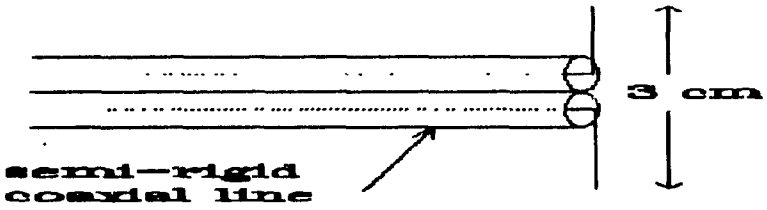

Figure A.7

Originally, the two conductors were to be fed to a wideband operational amplifier which would take care of the phase shifting while providing much needed amplification to an inherently weak signal. Unfortunately, op-amp chips providing the proper combination of low noise, wide bandwidth, high gain and large dynamic range could not readily be found as a stock item from commercial suppliers.

An alternative solution was found, using 180° combiners to take care of the phase shifting. A phase shifting combiner is a three port device that adds the input A to the phase shifted input B and presents the sum at output C. Although these devices introduce a 2 dB loss, their high dynamic range, low noise and broad bandwidth made them the most practical choice for this stage of the project. Three combiners were used, one for each dipole, such that three outputs had to be measured to get the three components of the electric field.

A.5 Conclusion

The result is a small, maneuverable, isotropic (by virtue of its feeding arrangement), broadband (the bandwidth is determined by the receiving instrument's noise floor) electric field probe capable of sensing three orthogonal components of the Electric field vector.

A.6 Measuring system specifications

As a consequence of the experience gained in the measurements using the above described sensing probe and the available measuring instruments, it is possible to write a set of specifications on the basis of which operational measuring equipment of this type can be designed, developed and constructed. Such equipment would be useful both for survey and monitoring purposes. The specifications of such a measurement system follow.

The system must be able to measure and store all three signals from the probe simultaneously. It must be portable (or at the very least, mobile), require very little power and be autonomous (battery operated). Eventually, it should be able to move on its own, either under remote control or according to a preprogrammed path (i.e. on a robotic carriage).

The reasons behind the above specifications are simple. All three signals are to be measured simultaneously so as to reduce the error due to the time variations in the

signals. The system should therefore include three measuring instruments (spectrum analyzers or receivers), and the coordination of the three would be left to a laptop computer. The receiving equipment must be sensitive enough to measure moderate electric fields with the probe. The computer would not only control the operation of the measuring instruments, but also acquire the data, process it to obtain the vector sum of the three E field components and save it on appropriate medium. Eventually, the same computer would control the movements of the probe, therefore easing the task of making detailed surveys of the field structure inside a room. The space limitations and the uncertainty associated with finding electrical outlets call for the system to be small, mobile, frugal and autonomous.

Appendix B EQUIVALENT ELECTRIC FIELDS IN EACH ROOM

The equivalent electric fields for each of the rooms surveyed are reported here. All values are in dBμV/m and a 0 indicates a band that has not been measured. The rooms are in no particular order, save that they are grouped by hospital.

Table B.1

Equivalent electric field on the eighth floor of hospital D, within view of the main transmitter tower on Mount Royal. This room was empty because the department which had used it previously moved to a newer wing in part because of interference.

bands	predicted	measured by DOC	measured by McGill
0-30 MHz	106	0	0
30-50 MHz	100	92	0
138-174 MHz	102	91	0
400-470 MHz	103	100	0
806-890 MHz	105	100	0
fm band	121	110	97

Table B.2

Equivalent electric field in a critical care area on the third floor of hospital D.

band	predicted	measured by DOC	measured by McGill
0-30 MHz	106	0	0
30-50 MHz	100	80	0
138-174 MHz	102	83	0
400-470 MHz	103	85	0
806-890 MHz	105	107	0
fm band	121	97	95

Table B.3

Equivalent electric field in a critical care area on the fifth floor of hospital D. Case room recovery room, very near the room where an incubator malfunctioned due to the EMI caused by a security person's handheld transceiver.

band	predicted	measured by DOC	measured by McGill
0-30 MHz	106	0	0
30-50 MHz	100	92	0
138-174 MHz	102	88	0
400-470 MHz	103	79	0
806-890 MHz	105	102	0
fm band	121	93	80

Table B.4

Equivalent electric field outside the main entrance of hospital D.

band	predicted	measured by DOC	measured by McGill
0-30 MHz	106	0	0
30-50 MHz	100	106	0
138-174 MHz	102	101	0
400-470 MHz	103	102	0
806-890 MHz	105	101	0
fm band	121	111	0

Table B.5

Equivalent electric field on the second floor of hospital D. This room was partially shielded by a metallic vapor barrier.

band	predicted	measured by DOC	measured by McGill
0-30 MHz	106	0	0
30-50 MHz	100	61	0
138-174 MHz	102	60	0
400-470 MHz	103	60	0
806-890 MHz	105	50	0
fm band	121	72	72

Table B.6

Equivalent electric field in a critical care area on the second floor of hospital D. This room was within the core of the building.

band	predicted	measured by DOC	measured by McGill
0-30 MHz	106	0	0
30-50 MHz	100	87	0
138-174 MHz	102	80	0
400-470 MHz	103	75	0
806-890 MHz	105	91	0
fm band	121	85	83

Table B.7

Equivalent electric field a diagnostic laboratory on the thirteenth floor of hospital C, in direct view of the broadcast transmitter towers in Montreal.

band	predicted	measured by DOC	measured by McGill
0-30 MHz	107	0	0
30 50 MHz	96	74	0
138-174 MHz	121	91	0
400-470 MHz	112	89	0
806-890 MHz	114	84	0
fm band	128	115	111

Table B.8

Equivalent electric field outside the main entrance of hospital C.

band	predicted	measured by DOC	measured by McGill
0-30 MHz	107	0	0
30-50 MHz	96	66	0
138-174 MHz	118	96	0
400-470 MHz	112	84	0
806-890 MHz	114	104	0
fm band	128	120	0

Table B.9

Equivalent electric field in a critical care area on the ninth floor of hospital C, in direct view of the towers, where radiant heaters for neonatal care had previously malfunctioned due to the ambient EME.

band	predicted	measured by DOC	measured by McGill
0-30 MHz	107	0	0
30-50 MHz	96	79	0
138-174 MHz	120	93	0
400-470 MHz	112	77	0
806-890 MHz	114	94	0
fm band	128	120	113

Table B.10

Equivalent electric field across the hall from the room described in table B.9. This room was shadowed by the building.

band	predicted	measured by DOC	measured by McGill
0-30 MHz	107	0	0
30-50 MHz	96	72	0
138-174 MHz	120	83	0
400-470 MHz	112	72	0
806-890 MHz	114	95	0
fm band	128	105	0

Table B.11

Equivalent electric field in a diagnostic laboratory on the fourth floor of hospital C, in direct view of the towers, where an automated laboratory machine malfunctioned due to EMI.

band	predicted	measured by DOC	measured by McGill
0-30 MHz	107	0	0
30-50 MHz	96	67	0
138-174 MHz	119	94	0
400-470 MHz	112	78	0
806-890 MHz	114	87	0
fm band	128	113	113

Table B.12

Equivalent electric field across the hall from the room described in table B.11, where the automated laboratory device was moved and then functioned normally.

band	predicted	measured by DOC	measured by McGill
0-30 MHz	107	0	0
30-50 MHz	96	60	0
138-174 MHz	119	69	0
400-470 MHz	112	63	0
806-890 MHz	114	86	0
fm band	128	95	0

Table B.13

Equivalent electric field in another critical care area on the ninth floor of hospital C, in direct view of the towers.

band	predicted	measured by DOC	measured by McGill
0-30 MHz	107	0	0
30-50 MHz	96	64	0
138-174 MHz	120	88	0
400-470 MHz	112	83	0
806-890 MHz	114	91	0
fm band	128	114	121

Table B.14

Equivalent electric field down the hall from the room described in table B.13. The location described in this table was shadowed by the building.

band	predicted	measured by DOC	measured by McGill
0-30 MHz	107	0	0
30-50 MHz	96	60	0
138-174 MHz	120	84	0
400-470 MHz	112	72	0
806-890 MHz	114	106	0
fm band	128	104	0

Table B.15

Equivalent electric field on the eleventh floor of hospital A. The fifth floor of hospital A is at ground level on the side of the transmitter tower on Mount Royal.

band	predicted	measured by DOC	measured by McGill
0-30 MHz	106	0	0
30-50 MHz	108	68	0
138-174 MHz	115	89	0
400-470 MHz	122	79	0
806-890 MHz	120	94	0
fm band	128	104	0

Table B.16

Equivalent electric field in a critical care area on the fourteenth floor of hospital A.

band	predicted	measured by DOC	measured by McGill
0-30 MHz	106	0	0
30-50 MHz	108	61	0
138-174 MHz	115	84	0
400-470 MHz	122	77	0
806-890 MHz	120	97	0
fm band	128	117	133

Table B.17

Equivalent electric field in a critical care area on the fifth floor of hospital A.

band	predicted	measured by DOC	measured by McGill
0-30 MHz	106	0	0
30-50 MHz	108	60	0
138-174 MHz	115	74	0
400-470 MHz	122	59	0
806-890 MHz	120	60	0
fm band	127	106	0

Table B.18

Equivalent electric field in an area adjacent to a critical care area on the eighth floor of hospital A.

band	predicted	measured by DOC	measured by McGill
0-30 MHz	106	0	0
30-50 MHz	108	66	0
138-174 MHz	115	81	0
400-470 MHz	122	70	0
806-890 MHz	120	69	0
fm band	128	115	120

Table B.19

Equivalent electric field on the fifth floor of hospital A facing the tower. This survey was done prior to the installation of new radiology facilities.

band	predicted	measured by DOC	measured by McGill
0-30 MHz	106	0	0
30-50 MHz	108	63	0
138-174 MHz	114	82	0
400-470 MHz	122	75	0
806-890 MHz	120	74	0
fm band	127	109	119

Table B.20

Equivalent electric field outside hospital A.

band	predicted	measured by DOC	measured by McGill
0-30 MHz	106	0	0
30-50 MHz	108	72	0
138-174 MHz	114	100	0
400-470 MHz	122	91	0
806-890 MHz	120	98	0
fm band	128	118	0

Table B.21

Equivalent electric field on the roof of hospital A.

band	predicted	measured by DOC	measured by McGill
0-30 MHz	106	0	0
30-50 MHz	108	104	0
138-174 MHz	115	101	0
400-470 MHz	122	97	0
806-890 MHz	120	99	0
fm band	128	136	137

Endnotes

1. Frank, V.A. And Lodner, R.T., "The Hospital Electromagnetic Interference Environment," Journal of the Association for the Advancement of medical Instrumentation, Vol. 5, No. 4, August 1971, pages 246-254

2. Toler, J.C., "Electromagnetic Interference Levels in Hospitals," 1975 IEEE EMC Symposium, San Antonio, Texas, 7-9 Oct., 1975, page 5BIIe/1

3. Hoff, R.J., "EMC Measurements in Hospitals," 1975 IEEE EMC Symposium, San Antonio, Texas, 7-9 Oct., 1975, page 5BIIc/1-5

4. Ruggera, P.S. "Radiofrequency E-Field Measurements in a Hospital Environment," IEEE EMC Symposium, San Antonio, Texas, 7-9 Oct., 1975, page 5BIId/1-3

5. FDA MDS 201 0004 1979, "Electromagnetic Compatibility Standard For Medical Devices," published by the US Department of Health, Education and Welfare, Food and Drug Administration, Bureau of Medical Devices.

6. Proceedings of the Workshop on Electromagnetic Interference and Electromagnetic Compatibility in Health Care Facilities, Edmonton, Alberta, November 18 and 19, 1987, published by the Electronics Test Center, Edmonton, Alberta

7. IEEE std 473-1985, "Recommended Practice for an Electromagnetic Site Survey (10 kHz to 10 GHz)"

8. "Measuring the Radio Frequency Environment", Skomal, E.N., And Smith, A.A., Van Nostrand Reinhold, 1985

9. Kanda & Ries, "A Broadband, Isotropic, Real Time Electric Field Sensor (BIRES) Using Resistively Loaded Dipoles", IEEE trans on EMC, vol. EMC-23, no. 3, August 1981, pages 122-132.

10. Pavlasek, Banik, Kaliouby and LeBel, "The Urban Electromagnetic Environment in Canadian Cities", Canadian Conference on Electrical and Computer Engineering, Vancouver, B.C., Canada, November 3-4, 1988

11. Al-Mahdawi, T.I. And Pavlasek, T.J.F.,"Wire and Aperture Probe Modelling in Planar Near-Field Scanning", Antem 90, Winnipeg, August 15-17, 1990

12. Banik, Pavlasek and LeBel, "Electric Field Strength Surveys of Broadcast Signals in an Urban Environment", International Conference on Electromagnetic Interference and Compatibility, Bangalore, India, 10-11 Sept, 1987, 341-344

13. Antennas, Kraus, John D., McGraw Hill, 1988